

# NIPM-HLSP: An Efficient Interior-Point Method for Hierarchical Least-Squares Programs

Kai Pfeiffer<sup>1</sup>, Adrien Escande<sup>2,3</sup>, Ludovic Righetti<sup>1</sup>

**Abstract**—Hierarchical least-squares programs with linear constraints (HLSP) are a type of optimization problem very common in robotics. Each priority level contains an objective in least-squares form which is subject to the linear constraints of the higher priority hierarchy levels. Active-set methods (ASM) are a popular choice for solving them. However, they can perform poorly in terms of computational time if there are large changes of the active set. We therefore propose a computationally efficient primal-dual interior-point method (IPM) for HLSP's which is able to maintain constant numbers of solver iterations in these situations. We base our IPM on the null-space method which requires only a single decomposition per Newton iteration instead of two as it is the case for other IPM solvers. After a priority level has converged we compose a set of active constraints judging upon the dual and project lower priority levels into their null-space. We show that the IPM-HLSP can be expressed in least-squares form which avoids the formation of the quadratic Karush-Kuhn-Tucker (KKT) Hessian. Due to our choice of the null-space basis the IPM-HLSP is as fast as the state-of-the-art ASM-HLSP solver for equality only problems.

## I. INTRODUCTION

### A. Hierarchical control in robotics

Hierarchical control is a well established and well-used methodology in robotics. It allows the full exploitation of the robot's kinematic redundancy resulting in increased dexterity and versatility [1]. Furthermore, it helps reflecting the physical reality of the robot as accurately as possible. An example would be to separate the equation of motion from self-collision or geometrical contact constraints by defining them on different priority levels [2], [3]. Prioritized controllers also exhibit a high level of safety since they enable to strictly separate safety constraints, physical stability constraints and objective tasks.

Starting with the seminal work of [1], the authors proposed an efficient way of computing a hierarchical control law where each task is only fulfilled to such a degree that the performance of higher priority tasks is not influenced. The authors in [4] proposed a similar approach but avoid the issue of algorithmic singularities which arise when a task is in conflict with a higher priority one. These methods have been successfully implemented for both velocity [5] and torque [6] controlled

robots. However, they do not enable the incorporation of inequality constraints like joint limits [7], collision avoidance [8] or visibility [9]. The integration of such tasks by means of a potential function on the highest priority level has been proposed [10] but this boils down to a reformulation to an equality constraint. For a continuous formulation without switches of priority order [11] this means that the constraint is always active and may negatively influence the robot control performance. With the rise of optimization based control approaches in robotics however, in particular least-squares (LSP) programming [12]–[15], several works have been presented to provide a framework to incorporate inequality constraints. The authors in [11] solve each level of the priority as its own optimization problem. Introducing slack variables enables the incorporation of inequality constraints on any priority level. A big disadvantage of this approach is that each optimization problem grows in the number of constraints since the ones from the previous levels need to be considered. In [16] this is avoided by only considering feasible inequality constraints on the first level. By solving each level in the null-space of the previous ones the problem dimensions are progressively reduced. The approach considered in [17] is also based on such a formulation of the null-space method but enables the incorporation of inequality constraints on any priority level. Unlike the previous cascade-like approaches [11], [16] their active-set search solves the whole hierarchy at once which adds further efficiency by unifying the search of all the levels into one. The latest dedicated solver for hierarchical least-squares programs proposes the use of non-orthogonal bases of the null-space which exposes a computationally efficient block structure [18].

### B. The hierarchical active-set method

A hierarchical LSP with linear constraints (HLSP) is an optimization problem which is not limited to a single least squares objective with linear constraints but is extended to an arbitrary number of priority levels. Each level consists of a least squares objective which is subject to the linear constraints of the higher priority levels. In the sense of [11] such an optimization problem boils down to the following form

$$\begin{aligned}
 \min_{x, v_{l,e}, v_{l,i}} \quad & \frac{1}{2} \|v_{l,e}\|^2 + \frac{1}{2} \|v_{l,i}\|^2 \quad l = 1, \dots, p \\
 \text{s.t.} \quad & A_{l,e}x - b_{l,e} = v_{l,e} \\
 & A_{l,i}x - b_{l,i} \geq v_{l,i} \\
 & \underline{A}_{l-1,e}x - \underline{b}_{l-1,e} = v_{l-1,e}^* \\
 & \underline{A}_{l-1,i}x - \underline{b}_{l-1,i} \geq 0
 \end{aligned} \tag{1}$$

<sup>1</sup>Machines in Motion Laboratory, Tandon School of Engineering, New York University, New York, USA

<sup>2</sup>CNRS-AIST JRL (Joint Robotics Laboratory), IRL, Tsukuba, Japan

<sup>3</sup>National Institute of Advanced Industrial Science and Technology (AIST), Tsukuba, Japan

Part of this work was supported by New York University, NSF grants 1936332, 1824434, 1833666, 1564142, 1925079, 1825993; NYU WIRELESS and its industrial affiliates; NIST grant 70NANB17H166; SRC; and a research grant from OPPO.

The variable vector  $x \in \mathbb{R}^n$  consists of  $n$  variables. The slack variables  $v_{l,e}$  and  $v_{l,i}$  relax the equality and inequality constraints  $A_{l,e}$  and  $A_{l,i}$  of the current level  $l$ . This relaxation allows handling of inequality and infeasible constraints on any priority level [19]. The hierarchy is resolved in a cascade-like manner from the first to the last level  $p$  while not violating the inequality constraints  $\underline{A}_{l-1,i}$  and not changing the optimal relaxation  $\underline{v}_{l-1,e}^*$  identified for the equality constraints  $\underline{A}_{l-1,e}$  of the previous levels. Underlined matrices and vectors are concatenations of the form  $\underline{M}_{l-1} = [M_1^T \ \cdots \ M_{l-1}^T]^T$ .

The dedicated solvers for HLSP's [17], [18] are both based on the ASM. At each solver iteration an equality only problem consisting of all equality constraints and the active inequality constraints  $\underline{A}_{l-1}$  from the lower priority levels 1 to  $l-1$  is solved. The most violated constraint of all the priority levels is then added to the active set. If all constraints are feasible, the dual is evaluated and the constraint preventing progression towards the optimal the most is removed. The ASM converges if no constraint needs to be added to or removed from the active set. In ASM's based on the null-space method the objective matrix  $A_l$  is projected into the null-space of the active constraints  $\underline{A}_{l-1}$  [20], [21]. With the right choice of null-space basis this leads to a possibly significant reduction of variables especially on lower priority levels in case of a large number of linearly independent active constraints. This makes the solvers very efficient. While [17] uses orthogonal bases the authors in [18] implement non-orthogonal bases with a further computational advantage due to their block structure. To the best of our knowledge, it is the state-of-the-art HLSP solver and is most efficient on problems which can be warm-started with a limited number of active-set iterations. For this solver some computational improvements have been proposed [22] in order to efficiently handle significant changes of the active-set. However, a strategy for decomposition updates, which would bring significant computational improvements in case of large number of active set iterations, has yet to be proposed.

The ASM is only computationally tractable if there are limited changes of the active set. This is usually the case for slowly developing robot problems (from a control rate perspective) and can be especially leveraged by warm starting the active set  $\mathcal{A}^{(i)}$  of the current control iteration  $i$  with the active set  $\mathcal{A}^{(i-1)}$  of the previous control iteration  $i-1$  [23]. However, in robotic real-time control there are cases where large shifts of the active set occur like in instances close to contact shifting or oscillations in case of numerical instabilities due to ill-posed constraint matrices. In these cases the convergence rate of the ASM may be exponential in the number of constraints as all possible active-set combinations need to be explored [24]. In the robotics control case this may occur in the presence of kinematic or algorithmic singularities [4] (an efficient way of resolving such singularities in the kinematic and dynamic hierarchical control case has been proposed in [25], [26]). Numerical issues like cycling can further increase the number of active set iterations such that it becomes intractable for real-time robot control. While methods mitigating such effects like decomposition updates [27] and cycling handling [28] exist, they might not be enough to make up for the possibly large

number of active set iterations until convergence [26].

This is in contrast to the IPM where all constraints including inactive inequality constraints are included. Consequently, a single iteration of the IPM is relatively expensive but convergence is achieved robustly in a deterministic number of iterations independent of conditioning [29], [30]. The authors in [31] for example use this circumstance and switch from the fast ASM to the reliable IPM in case of ASM failures. The IPM is more suitable for large scale problems with a large number of variables and constraints while for small scale problems the ASM is usually preferred [32]. This also applies to a further method of resolving QP's, the Alternating Direction Method of Multipliers (ADMM) [33], [34]. This operator-splitting method has very good practical convergence behavior, warm-start capabilities and low iteration cost. While the solver is not designed to converge at high accuracy, it has been recently proposed to derive active set guesses from intermediate solver states and solve the corresponding equality only problem [35]. If the active-set guess is correct the solution has zero primal and dual residual. The same framework also overcomes tuning difficulties associated with operator-splitting methods and requires only a single factorization for solving the QP, making it very fast especially for large-scale problems.

### C. Our contribution

While the IPM has been developed for LSP [36] and could be used to solve (1) directly, there exist no dedicated IPM (or ADMM thereof) based solvers for HLSP. In this work we will provide the theoretical foundations to achieve just that. Our IPM-HLSP formulation is as fast as the state-of-the-art ASM-HLSP solver [18] in case of equality only problems. At the same time the IPM based HLSP solver provides predictability in terms of computation times due to its constant number of Newton iterations even in case of ill-posed constraints matrices. Here the ASM-HLSP oftentimes requires large number of active set iterations and is therefore superseded by the IPM-HLSP. This can also be relevant when critical safety constraints need to be dealt with but the ASM-HLSP fails to find an optimal point in a reasonable number of active set iterations.

Our contributions are threefold:

- With our first contribution we formulate the IPM for HLSP. We thereby propose a HLSP solver purely based on the IPM but also present a solver design that is a combination of both the IPM and the ASM which utilizes the advantages of both schemes - that is reliability and fastness.
- We suggest to apply the null-space method to the IPM for HLSP instead of the commonly used Schur complement [37], [38]. While this has been previously done for QP's in MPC [39] we give a more detailed explanation for example on our choice of null-space basis. With this formulation we reduce the necessary number of decompositions of the KKT system per Newton iteration from two to one. Furthermore, the number of times the Lagrange multipliers associated with the equality constraints are evaluated can be reduced significantly with a special convergence test.

- We show that the projected normal equations of the IPM-HLSP can be expressed in least squares form. This way the formation of expensive matrix products is avoided and a basic solution can be very efficiently computed by a cheap QR decomposition.

This paper is structured as follows: In sec. II we first introduce the notion of active sets into the optimization problem (1). We then continue to outline the formulation of the IPM-HLSP and the corresponding hierarchical augmented system. Section III oversees the efficient computation of the IPM solver iterations. We apply the null-space method to the augmented system which results in the projected normal equations, sec. III-A. This requires a concept we refer to as virtual priority levels and which is detailed in sec. III-B. The choice of null-space basis is given in sec. III-C. With a special convergence test the calculation of the dual associated with the equality constraints in every Newton iteration can be avoided (sec. III-D). In sec. III-E the projected normal equations are expressed as a least squares problem. Section III-F oversees the development of Mehrotra’s predictor-corrector-algorithm for HLSP’s. Bound constraints can be specially handled by a sparse QR decomposition (sec. III-E2) for a more computationally efficient algorithm which is finally outlined in sec. IV. Finally, we give a computational comparison between the classical and projected normal equations and the least squares form (sec. V). The proposed algorithms are evaluated in sec. VI. We conclude the paper with some remarks and considerations for future work (see sec. VII).

The solver is open source and its C++ code based on the Eigen library [40] is available at <https://www.github.com/pfeiffer-kai/NIPM-HLSP>.

## II. FORMULATING THE IPM-HLSP

First, we look at the top three lines of the above optimization problem (1). This problem corresponds to finding a *feasible point* ( $v_{l,e}^* = 0, v_{l,i}^* \geq 0$ ) or *optimal infeasible point* ( $v_{l,e}^* \neq 0, v_{l,i}^* < 0$ ) of the constraints. In the context of linear programming the self-dual embedding model [41] has been proposed. Just like [37] for quadratic programming, infeasible initial points with respect to the equality constraints are handled but inequality constraints are assumed to be feasible with  $A_{l,i}x - b_{l,i} \geq 0$ . An algorithm overcoming this issue is proposed in [23] where the initial feasible point is determined by minimizing the sum of infeasibilities. However, the algorithm fails when no feasible but only an optimal infeasible point  $A_{l,i}x - b_{l,i} < 0$  exists. The solvers proposed in [17]–[19] are based on the ASM and are able of handling all above cases.

We rewrite (1), which is only valid if all inequality constraints on all levels are feasible, to

$$\begin{aligned} \min_{x, v_{l,e}, v_{l,i}} \quad & \frac{1}{2} \|v_{l,e}\|^2 + \frac{1}{2} \|v_{l,i}\|^2 \quad l = 1, \dots, p \quad (2) \\ \text{s.t.} \quad & A_{l,e}x - b_{l,e} = v_{l,e} \\ & A_{l,i}x - b_{l,i} \geq v_{l,i} \\ & \underline{A}_{\underline{A}_{l-1}} x - \underline{b}_{\underline{A}_{l-1}} = \underline{v}_{\underline{A}_{l-1}}^* \\ & \underline{A}_{\underline{A}_{l-1}^\#} x - \underline{b}_{\underline{A}_{l-1}^\#} \geq 0 \end{aligned}$$

The active set  $\underline{A}_{l-1}$  represents all equality constraints and the inequality constraints that were infeasible and violated by  $v_{\underline{A}_{l-1}}^*$  at the optimal points of the levels 1 to  $l-1$ . Consequently,  $\underline{A}_{\underline{A}_{l-1}^\#}$  are the remaining inequality constraints that were feasible and satisfied at the optimal points of the levels 1 to  $l-1$  and which are labeled as ‘inactive’ ( $\underline{A}_{\underline{A}_{l-1}^\#}$ ). More details on sourcing these active sets are given in sec. III-B.

The aim of the optimization problem is now

- to keep the previous levels  $1, \dots, l-1$  optimal at the current violation  $v_{\underline{A}_{l-1}}^* \rightarrow$  **Null-space method**
- to keep the inactive inequality constraints feasible  $\underline{A}_{\underline{A}_{l-1}^\#} x - \underline{b}_{\underline{A}_{l-1}^\#} \geq 0 \rightarrow$  **IPM**
- while finding the feasible or optimal infeasible point  $v_{l,i}^*$  and  $v_{l,e}^*$  of the  $l$ -th level  $\rightarrow$  **IPM** or **ASM**.

The first point is outlined in the next section III-A. The second and third point we intend to achieve by the IPM. The third point can equally be achieved by the ASM as is explained in Appendix E. While very good behavior is achieved in practice mathematical proof of convergence may be required for the overlay of the IPM with the ASM. Therefore, throughout this paper we focus on the pure IPM-HLSP formulation but include the IPM-ASM-HLSP into our evaluation which proves to be superior in terms of computation times with respect to the pure IPM-HLSP formulation.

We introduce two positive slack variables  $w_{l,i}$  for the inequality constraints on the current level  $l$  and  $\underline{w}_{\underline{A}_{l-1}^\#}$  for the inactive inequality constraints of the previous levels. They are then bounded away from zero by the log-barrier function:

$$\begin{aligned} \min_x \quad & \frac{1}{2} \|v_{l,e}\|^2 + \frac{1}{2} \|v_{l,i}\|^2 - \sigma_{l,i} \mu_{l,i} \sum \log(w_{l,i}) \quad (3) \\ & - \sigma_{\underline{A}_{l-1}^\#} \mu_{\underline{A}_{l-1}^\#} \sum \log(\underline{w}_{\underline{A}_{l-1}^\#}) \\ \text{s.t.} \quad & A_{l,e}x - b_{l,e} = v_{l,e} \\ & A_{l,i}x - b_{l,i} - v_{l,i} = w_{l,i} \\ & w_{l,i} \geq 0 \\ & \underline{A}_{\underline{A}_{l-1}} x - \underline{b}_{\underline{A}_{l-1}} = \underline{v}_{\underline{A}_{l-1}}^* \\ & \underline{A}_{\underline{A}_{l-1}^\#} x - \underline{b}_{\underline{A}_{l-1}^\#} = \underline{w}_{\underline{A}_{l-1}^\#} \\ & \underline{w}_{\underline{A}_{l-1}^\#} \geq 0 \end{aligned}$$

The Lagrangian of the optimization problem (3) writes as

$$\begin{aligned} \mathcal{L} = & \frac{1}{2} \|v_{l,e}\|^2 + \frac{1}{2} \|v_{l,i}\|^2 \quad (4) \\ & - \sigma_{l,i} \mu_{l,i} \sum \log(w_{l,i}) - \sigma_{\underline{A}_{l-1}^\#} \mu_{\underline{A}_{l-1}^\#} \sum \log(\underline{w}_{\underline{A}_{l-1}^\#}) \\ & - \lambda_{l,e}^T (A_{l,e}x - b_{l,e} - v_{l,e}) - \lambda_{l,i}^T (A_{l,i}x - b_{l,i} - v_{l,i} - w_{l,i}) \\ & - \underline{\lambda}_{\underline{A}_{l-1}}^T (\underline{A}_{\underline{A}_{l-1}} x - \underline{b}_{\underline{A}_{l-1}} - \underline{v}_{\underline{A}_{l-1}}^*) \\ & - \underline{\lambda}_{\underline{A}_{l-1}^\#}^T (\underline{A}_{\underline{A}_{l-1}^\#} x - \underline{b}_{\underline{A}_{l-1}^\#} - \underline{w}_{\underline{A}_{l-1}^\#}) \end{aligned}$$

The Lagrange multipliers associated with the inactive inequality constraints of the higher priority levels  $1, \dots, l-1$  are  $\underline{\lambda}_{\underline{A}_{l-1}^\#}$  ( $\underline{\Lambda}_{\underline{A}_{l-1}^\#} = \text{diag}(\underline{\lambda}_{\underline{A}_{l-1}^\#})$ ).

The first order optimality or KKT conditions  $\nabla_q \mathcal{L} = 0$  with the variable vector  $q$

$$q := \begin{bmatrix} x^T & v_{l,e}^T & v_{l,i}^T & w_{l,i}^T & \underline{\lambda}_{\underline{A}_{l-1}}^T & \underline{\lambda}_{\underline{A}_{l-1}^\#}^T & \underline{w}_{\underline{A}_{l-1}^\#}^T \end{bmatrix}^T \quad (5)$$

are (in a slightly rewritten form)

$$K_l := [k_{l,1}^T \quad k_{l,2}^T \quad k_{l,3}^T \quad k_{l,4}^T \quad k_{l,5}^T \quad k_{l,6}^T \quad k_{l,7}^T]^T = \quad (6)$$

$$\begin{bmatrix} A_{l,e}^T v_{l,e} + A_{l,i}^T v_{l,i} - \underline{A}_{\underline{A}_{l-1}}^T \lambda_{\underline{A}_{l-1}} - \underline{A}_{\underline{A}_{l-1}^\#}^T \lambda_{\underline{A}_{l-1}^\#} \\ b_{l,e} - A_{l,e}x + v_{l,e} \\ b_{l,i} - A_{l,i}x + v_{l,i} + w_{l,i} \\ w_{l,i} \odot v_{l,i} + \sigma_{l,i} \mu_{l,i} e \\ \underline{b}_{\underline{A}_{l-1}} - \underline{A}_{\underline{A}_{l-1}}x + \underline{v}_{\underline{A}_{l-1}}^* \\ \underline{b}_{\underline{A}_{l-1}^\#} - \underline{A}_{\underline{A}_{l-1}^\#}x + \underline{w}_{\underline{A}_{l-1}^\#} \\ \lambda_{\underline{A}_{l-1}^\#} \odot \underline{w}_{\underline{A}_{l-1}^\#} - \sigma_{\underline{A}_{l-1}^\#} \mu_{\underline{A}_{l-1}^\#} e \end{bmatrix} = 0$$

with the substitutions  $v_{l,e} = -\lambda_{l,e}$  and  $v_{l,i} = -\lambda_{l,i}$ .

The duality measures  $\mu$  and the centering parameters  $\sigma$  [42] are given by

$$\mu_{l,i} = \lambda_{l,i}^T w_i / (n + m_{l,i}) = -v_{l,i}^T w_i / (n + m_{l,i}) \quad (7)$$

$$\mu_{\underline{A}_{l-1}^\#} = \lambda_{\underline{A}_{l-1}^\#}^T \underline{w}_{\underline{A}_{l-1}^\#} / (n + \underline{m}_{\underline{A}_{l-1}^\#}) \quad (8)$$

$$\sigma_{l,i}, \sigma_{\underline{m}_{\underline{A}_{l-1}^\#}} \in [0, 1] \quad (9)$$

or the values can be determined by Mehrotra's predictor-corrector algorithm [43], see sec. III-F.

Additionally, we have the dual feasibility conditions which are ensured by line search. The IPM for finding the initial feasible or optimal infeasible point requires

$$v_{l,i} \leq 0 \quad \text{and} \quad w_{l,i} \geq 0 \quad (10)$$

For the IPM of the inactive constraints we have

$$\lambda_{\underline{A}_{l-1}^\#} \geq 0 \quad \text{and} \quad \underline{w}_{\underline{A}_{l-1}^\#} \geq 0 \quad (11)$$

The KKT conditions are non-linear so we apply the Newton step

$$K_l(q + \Delta q) \approx K_l(q) + \nabla_q K_l(q) \Delta q \quad (12)$$

with the KKT Hessian

$$\nabla_q K_l(q) := \quad (13)$$

$$\begin{bmatrix} 0 & A_{l,e}^T & A_{l,i}^T & 0 & -\underline{A}_{\underline{A}_{l-1}}^T & -\underline{A}_{\underline{A}_{l-1}^\#}^T & 0 \\ -A_{l,e} & I & 0 & 0 & 0 & 0 & 0 \\ -A_{l,i} & 0 & I & I & 0 & 0 & 0 \\ 0 & 0 & W_{l,i} & V_{l,i} & 0 & 0 & 0 \\ -\underline{A}_{\underline{A}_{l-1}} & 0 & 0 & 0 & 0 & 0 & 0 \\ -\underline{A}_{\underline{A}_{l-1}^\#} & 0 & 0 & 0 & 0 & 0 & I \\ 0 & 0 & 0 & 0 & 0 & \underline{W}_{\underline{A}_{l-1}^\#} & \underline{\Lambda}_{\underline{A}_{l-1}^\#} \end{bmatrix}$$

We sequentially apply substitutions for  $\Delta v_{l,e}$ ,  $\Delta v_{l,i}$ ,  $\Delta \underline{w}_{\underline{A}_{l-1}^\#}$ ,  $\Delta w_{l,i}$  and  $\Delta \lambda_{\underline{A}_{l-1}^\#}$  which leads to the hierarchical augmented system

$$\begin{bmatrix} C_l & -\underline{A}_{\underline{A}_{l-1}}^T \\ -\underline{A}_{\underline{A}_{l-1}} & 0 \end{bmatrix} \begin{bmatrix} \Delta x \\ \Delta \lambda_{\underline{A}_{l-1}^\#} \end{bmatrix} = \begin{bmatrix} r_{l,1} \\ r_{l,2} \end{bmatrix} \quad (14)$$

with

$$C_l = A_{l,e}^T A_{l,e} + A_{l,i}^T (I + (V_{l,i} - W_{l,i})^{-1} W_{l,i}) A_{l,i} \quad (15)$$

$$+ \underline{A}_{\underline{A}_{l-1}}^T \underline{W}_{\underline{A}_{l-1}^\#}^{-1} \underline{\Lambda}_{\underline{A}_{l-1}^\#} \underline{A}_{\underline{A}_{l-1}^\#}$$

and the right hand side

$$r_1 = \underline{A}_{\underline{A}_{l-1}}^T \lambda_{\underline{A}_{l-1}} + \underline{A}_{\underline{A}_{l-1}^\#}^T F + A_{l,e}^T (b_{l,e} - A_{l,e}x) + A_{l,i}^T G \quad (16)$$

$$r_2 = \underline{A}_{\underline{A}_{l-1}}x - \underline{b}_{\underline{A}_{l-1}} - \underline{w}_{\underline{A}_{l-1}^\#} \quad (17)$$

$G$  and  $F$  are given by

$$F = \lambda_{\underline{A}_{l-1}^\#} + W_{\underline{A}_{l-1}^\#}^{-1} (\lambda_{\underline{A}_{l-1}^\#} \odot (\underline{b}_{\underline{A}_{l-1}^\#} - \underline{A}_{\underline{A}_{l-1}^\#}x)) \quad (18)$$

$$+ \sigma_{\underline{A}_{l-1}^\#} \mu_{\underline{A}_{l-1}^\#} e$$

$$G = b_{l,i} - A_{l,i}x + w_{l,i} \quad (19)$$

$$- (V_{l,i} - W_{l,i})^{-1} (\sigma_{l,i} \mu_{l,i} e + w_{l,i} \odot (A_{l,i}x - b_{l,i} - w_{l,i}))$$

respectively.

The Newton's method (14) of level  $l$  is now solved repeatedly until the norm of the KKT conditions  $\|K_l\|_2 < \epsilon$  (6) is below a certain threshold  $\epsilon = 10^{-12}$ .

### III. COMPUTING THE IPM-HLSP

#### A. The null-space method based IPM-HLSP

Solving the augmented system (14) directly is inefficient as the zero block in the lower right corner of the left hand side matrix would be ignored. One way to circumvent this is to form the Schur complement [38]

$$\Delta x = C_l^{-1} (r_{l,1} + \underline{A}_{\underline{A}_{l-1}}^T \Delta \lambda_{\underline{A}_{l-1}^\#}) \quad (20)$$

The resulting 'classical' normal equations are given below:

$$\underline{A}_{\underline{A}_{l-1}} C_l^{-1} \underline{A}_{\underline{A}_{l-1}}^T \Delta \lambda_{\underline{A}_{l-1}^\#} = -r_{l,2} - \underline{A}_{\underline{A}_{l-1}} C_l^{-1} r_{l,1} \quad (21)$$

This substitution yields a dense matrix  $\underline{A}_{\underline{A}_{l-1}} C_l^{-1} \underline{A}_{\underline{A}_{l-1}}^T$  and potential sparsity is destroyed [42]. This is especially relevant in robotics where the columns rather than the rows of  $\underline{A}_{\underline{A}_{l-1}}$  are zero when considering multi-limbed robots with tree-like structures. Additionally, in order to solve this system two decompositions per Newton iteration are required, one for  $C_l^{-1}$  and one for  $\underline{A}_{\underline{A}_{l-1}} C_l^{-1} \underline{A}_{\underline{A}_{l-1}}^T$ . Efficient strategies especially in the context of Model-Predictive-Control (MPC) leveraging banded matrix structures have been proposed [38]. However, we would like to avoid the computation of two decompositions per Newton iteration after all. First, we assume that Furthermore, in robotic control hierarchies,  $C_l$  is generally not full rank (unless it is a regularization term on some low priority level) which renders the classical normal equations not applicable for hierarchies (since  $C_l^{-1}$  can not be computed). In case that  $C_l$  is full rank, there might be linear dependent constraints in  $\underline{A}_{\underline{A}_{l-1}}$  at which point every Newton iteration requires a rank revealing decomposition for  $\underline{A}_{\underline{A}_{l-1}} C_l^{-1} \underline{A}_{\underline{A}_{l-1}}^T \in \mathbb{R}^{m_{\underline{A}_{l-1}}, m_{\underline{A}_{l-1}}} (O(4/3 m_{\underline{A}_{l-1}}^3))$  in case of QR decomposition).

However, we can avoid the computation of two decompositions per Newton iteration by first assuming that

$$r_{l,2} = 0 \quad (22)$$

This condition holds as  $x$  is updated after every Newton iteration during the resolution of the higher priority levels  $l = 1, \dots, l-1$  and is therefore feasible with respect to the

active constraints  $\underline{A}_{l-1}$ . The computation of  $r_{l,1}$  requires this step since it depends on the latest  $x$ . On the other hand, ASM-HLSP requires the evaluation of the new  $x$  only at the end of each active set iteration resolving the equality only HLSP.

We then apply the null-space method [44] by introducing the variable change

$$\Delta x = N_{l-1} \Delta z \quad (23)$$

The null-space basis  $N_{l-1}$  of  $\underline{A}_{A_{l-1}}$  fulfills the condition  $\underline{A}_{A_{l-1}} N_{l-1} = 0$ . Additionally,  $\underline{A}_{A_{l-1}} \Delta x = 0$  such that the condition  $r_{l,2} = 0$  continues to be fulfilled.

An additional multiplication of the first row of (14) by  $N_{l-1}^T$  from the left results in the projected hierarchical normal equations

$$N_{l-1}^T C_l N_{l-1} \Delta z = N_{l-1}^T r_{l,1} \quad (24)$$

The Lagrange multipliers  $\lambda_{A_{l-1}}$  corresponding to the active constraints  $\underline{A}_{l-1}$  are obtained by solving

$$\underline{A}_{A_{l-1}}^T \Delta \lambda_{A_{l-1}} = C_l \Delta x - r_{l,1} \quad (25)$$

An efficient recursive method of calculation is detailed in Appendix A.

### B. Notion of virtual priority levels

Once the Newton's method of a priority level  $l$  has converged constraints from  $\underline{A}_{A_l^\xi}$  are either saturated with  $\underline{A}_{A_l^\xi} x - \underline{b}_{A_l^\xi} = 0$  or satisfied with  $\underline{A}_{A_l^\xi} x - \underline{b}_{A_l^\xi} \geq 0$ . Additionally, inequality constraints from the current level  $l$  are either satisfied with  $A_{l,i} x - b_{l,i} \geq 0$  or violated with  $A_{l,i} x - b_{l,i} < 0$ . In order to be able to proceed with the cascade-like resolution of the next priority level we need to determine two distinct active sets  $\mathcal{A}_{l^*}$  and  $\mathcal{A}_l$  ( $\underline{A}_l = [\mathcal{A}_1^* \quad \mathcal{A}_1 \quad \dots \quad \mathcal{A}_l^* \quad \mathcal{A}_l]$ ). The index  $l^*$  represents a 'virtual' priority level whose active set  $\mathcal{A}_{l^*}$  contains saturated constraints from  $\underline{A}_{A_{l-1}^\xi}$ . This is necessary as the projection of  $\underline{A}_{A_{l-1}^\xi}$  into the null-space basis of the active constraints of level  $l$  would contradict the priority order. Therefore, a virtual priority level  $l^*$  has lower priority than level  $l-1$  but higher priority than level  $l$  which comprises of the equality constraints  $A_{l,e}$  and the activated constraints from  $A_{l,i}$ .

This also has the effect of reducing the size of  $\underline{A}_{A_{l-1}^\xi}$  while a significant null-space basis can be augmented which reduces the number of variables for the Newton's method of the next priority level for a cheaper algorithm.

We activate a constraint from  $\underline{A}_{A_{l-1}^\xi}$  if the corresponding pair of slack and Lagrange multiplier fulfills the conditions

$$\underline{w}_{A_{l-1}^\xi} < \xi \quad \text{and} \quad \underline{\lambda}_{A_{l-1}^\xi} > \xi \quad (26)$$

While  $\underline{w}_{A_{l-1}^\xi}(i) < \xi$  ensures that only saturated constraints are activated, the condition  $\underline{\lambda}_{A_{l-1}^\xi}(i) > \xi$  only selects constraints that are in significant conflict with constraints from level  $l$  and are not just accidentally saturated, for example by a randomly chosen initial point. Otherwise the ability of resolving the lower priority level  $l$  is artificially restricted by an unnecessarily inflated active set  $\underline{A}_{l-1}$ .

The thresholding  $\xi = 10^{-8}$  is necessary as the Newton's method is usually not run to complete convergence  $\|K_l\|_2 = 0$  but stopped earlier with some threshold  $\|K_l\|_2 < \epsilon$ . Note that our small choice for  $\xi$  requires the Newton's method to converge to a similarly accurate degree  $\epsilon = 10^{-12}$  in order to have an accurate value of the dual  $\underline{w}_{A_{l-1}^\xi}$  and  $\underline{\lambda}_{A_{l-1}^\xi}$ . In case that the Newton's method converges sub-optimally, we recalculate  $\underline{w}_{A_{l-1}^\xi} = \underline{A}_{A_{l-1}^\xi} x - \underline{b}_{A_{l-1}^\xi}$  explicitly which has a positive effect on the convergence of the lower priority levels (similarly for  $v_{l,i}$ ).

The following steps are then conducted for  $l^*$ :

- Add the newly activated constraints from  $\underline{A}_{l-1}^\xi$  to  $A_{l^*}$  as a 'virtual' priority level  $l^*$ .
- Calculate its null-space basis  $Z_{l^*}$  of  $A_{A_{l^*}} N_{l-1}$ .
- Continue  $N_{l-1}$  to  $N_{l^*} = N_{l-1} Z_{l^*}$

Now we handle the violated constraints from level  $l$  for the active set  $\mathcal{A}_l$  which are activated if the following conditions are fulfilled:

$$w_{l,i} < \xi \quad \text{and} \quad v_{l,i} < -\xi \quad (27)$$

The condition  $v_{l,i} < -\xi$  ensures that only significantly violated constraints are activated. The condition  $w_{l,i} < \xi$  sorts out constraints that are satisfied. Then following steps complete the active set assembly:

- Assemble the active set  $\mathcal{A}_l$  of level  $l$  with all equality constraints and the active inequality constraints.
- Inactive constraints are added to  $\underline{A}_l^\xi$ . Note that in the case of bound constraints we check whether the variable is already constrained by the same constraint. If this is the case no new constraint is added and the tighter bound of the two is used as the new right hand side  $\underline{b}_{A_l^\xi}$ . This prevents unnecessarily increasing the size of  $\underline{A}_{A_l^\xi}$ .
- Calculate the null-space basis  $Z_l$  of  $A_{A_l} N_{l^*}$ .
- Continue  $N_{l^*}$  to  $N_l = N_{l^*} Z_l$ .

Note that even though we assemble the null-space  $N_{l-1}$  step-wise like this we always have  $\underline{A}_{A_{l-1}} N_{l-1} = 0$ .

### C. Choice of null-space basis and variable elimination

For an overall cheap algorithm we require that

- The projection  $\tilde{M} = M N_l = M N_{l-1} Z_l$  reduces the number of variables of  $M$  depending on the number of linear independent constraints in  $A_{A_l}$ .
- The matrix product  $\tilde{M} = M N_{l-1} Z_l$  needs to be computed cheaply.
- The decomposition for computing  $Z_l$  should be reusable for the computation of the dual  $\underline{\lambda}_{A_l}$ .

The non-orthogonal basis

$$Z_l = P \begin{bmatrix} -R^{-1}T \\ I \end{bmatrix} \quad (28)$$

derived from the rank-revealing QR decomposition

$$A_{A_l} = Q \begin{bmatrix} R & T \\ 0 & 0 \end{bmatrix} P^T \quad (29)$$

fulfills all these requirements [18].  $Q$  is an orthogonal matrix,  $R$  is upper triangular,  $T$  is a rectangular matrix and  $P$  is a

permutation matrix. The bottom zero row is due to possible linear dependencies in  $A_{\mathcal{A}}$ .

If  $r_l = \text{rank}(A_{\mathcal{A}_l} N_{l-1})$  then its null-space  $Z_l \in \mathbb{R}^{n_r, n_r = n_r - r_l}$  and the same for  $N_l = N_{l-1} Z_l = Z_1 \cdots Z_l \in \mathbb{R}^{n_r, n_r = n_r - r_l}$ .  $n_r$  is the number of remaining variables of the current level  $l$ . We therefore solve increasingly smaller Newton's methods (24) as we descend the hierarchy by eliminating variables through the null-space projections. This scheme is therefore commonly referred to as variable elimination [45].

#### D. Avoiding the calculation of $\Delta \lambda_{\mathcal{A}_{l-1}}$

The cost of calculating the dual step  $\Delta \lambda_{\mathcal{A}_{l-1}}$  associated with the equality constraints  $A_{\mathcal{A}_{l-1}}$  is of magnitude  $O(r_{\mathcal{A}_{l-1}}^2)$ . The rank of  $A_{\mathcal{A}_{l-1}}$  is given as  $r_{\mathcal{A}_{l-1}}$ . However, we do not necessarily need to update the Lagrange multipliers  $\lambda_{\mathcal{A}_{l-1}}$  since none of the other primal or dual variables depend on them. Additionally, we can explicitly calculate  $\lambda_{\mathcal{A}_{l-1}}$  by solving  $k_{l,1} = 0$  (6). This is in contrast to the augmented system (14) or the classical normal equations (21) which require the calculation of the dual in order to obtain the primal.

The dual  $\lambda_{\mathcal{A}_{l-1}}$  is only necessary to calculate  $k_{l,1}$  for the evaluation of the norm of  $K_l$  (6) to determine whether the IPM has converged with  $\|K_l\|_2 < \epsilon$ . We can reduce the number of dual evaluations (25) with our adapted convergence test:

- Check whether  $\left\| \begin{bmatrix} k_{l,2}^T & \cdots & k_{l,7}^T \end{bmatrix}^T \right\|_2 < \epsilon$ .
- If this is the case solve  $k_{l,1} = 0$  (6) for  $\lambda_{\mathcal{A}_{l-1}}$ . Then calculate the residual  $k_{l,1}$  and do the convergence test  $\|K_l\|_2 < \epsilon$ .
- Otherwise,  $\lambda_{\mathcal{A}_{l-1}}$  and  $k_{l,1}$  are not evaluated.

#### E. The least-squares form of the IPM-HLSP

The HLSP (24) can be rewritten to least squares form as is demonstrated in Appendix B. The overall least-squares form of the IPM-HLSP then becomes

$$\min_{\Delta z} \left\| \begin{bmatrix} \sqrt{W_{\mathcal{A}_{l-1}^{\mathcal{A}_{l-1}}}^{-1} \tilde{A}_{\mathcal{A}_{l-1}^{\mathcal{A}_{l-1}}} \tilde{A}_{\mathcal{A}_{l-1}^{\mathcal{A}_{l-1}}}} \\ \sqrt{I + (V_{1,i} - W_{1,i})^{-1} W_{1,i} \tilde{A}_{l,i}} \\ \tilde{A}_{l,e} \end{bmatrix} \Delta z \right\|_2 \quad (30)$$

$$- \left\| \begin{bmatrix} \sqrt{W_{\mathcal{A}_{l-1}^{\mathcal{A}_{l-1}}}^{-1} F} \\ \sqrt{I + (V_{1,i} - W_{1,i})^{-1} W_{1,i} G} \\ b_{l,e} - A_{l,e} x \end{bmatrix} \right\|_2^2$$

$F$  and  $G$  are defined in (18) and (19), respectively. We use the notation  $\tilde{M} := M N_{l-1}$ .

Following our considerations from sec. V we use the condition

$$\underline{m}_{\mathcal{A}_{l-1}^{\mathcal{A}_{l-1}}} + m_{l,i} + 2m_{l,e} < 2n_r \quad (31)$$

to decide whether the least-squares form (30) is more appropriate than the projected normal equations (24) (assuming the use of a QR decomposition as the full rank condition of  $C_l$  is usually not fulfilled in hierarchies except for the last level  $p$ ).

In appendix C we present an efficient rank revealing QR decomposition (RRQR) of (30) leveraging the triangular structure of a pre-computed RRQR of  $A_{l,e} N_{l-1}$  which is constant over the course of the Newton's method.

#### 1) Accordance of the IPM-HLSP with the ASM-HLSP:

The least-squares form of the IPM-HLSP (30) clearly exposes the parallels with the ASM-HLSP. The IPM-HLSP considers the whole HLSP in each iteration of the IPM whereas the ASM-HLSP only considers active constraints while inactive constraints are ignored.

This means that for equality only problems ( $\underline{m}_{\mathcal{A}_{l-1}^{\mathcal{A}_{l-1}}} + m_{l,i} = 0$ ) the IPM-HLSP and the ASM-HLSP are identical:

$$\min_{\Delta z} \|A_{l,e} N_{l-1} \Delta z + (A_{l,e} x - b_{l,e})\|^2 \quad (32)$$

This corresponds to the least squares form of the ASM-HLSP formulated in [18] which can be considered the fastest way of resolving an equality only HLSP with performance rates similar to an LU decomposition of an equivalently weighted LSP.

#### 2) Handling bound constraints in the set of higher priority inactive constraints and the inequalities of the current level:

One disadvantage of the null-space method is that sparsity of the constraints is usually not maintained due to our choice of dense null-space basis. Nonetheless, some sparsity especially in the least squares form of the projected normal equation remains. We treat inactive bound constraints in  $\mathcal{A}_{\mathcal{A}_{l-1}^{\mathcal{A}_{l-1}}}$  and the inequalities of the current level  $A_{l,i}$  in a sparse manner. This can result in significant computational improvement especially in the robotics context where such constraints are common (joint limits, unilateral contact forces). We implement a sparse QR decomposition by zeroing sparse elements by Givens rotations. Tracking the sparsity comes basically for free as we can recognize sparse columns when computing the column norms during the rank revealing QR decomposition for the null-space calculation  $Z_{l^*}$  and  $Z_l$  of  $A_{\mathcal{A}_l^*} N_{l-1}$  and  $A_{\mathcal{A}_l} N_{l^*}$ . Zero columns of these matrices preserve sparse columns of  $\mathcal{A}_{\mathcal{A}_{l-1}^{\mathcal{A}_{l-1}}}$ ,  $\mathcal{A}_{\mathcal{A}_{l-1}^{\mathcal{A}_{l-1}}}$ ,  $A_{l,i} N_{l-1} Z_{l^*}$  and  $A_{l,i} N_{l^*} Z_l$ .

During stage 2 and stage 3 of our special RRQR (appendix C) we measure the density degree (number of dense entries / number of overall rows) of each sparse column (the further we advance the denser the remaining columns become). We apply Givens rotations as long as the density-degree is below a certain threshold (0.4, tuned manually). Otherwise we apply Householder transformations on the whole column neglecting the remaining sparsity since this proves to be faster due to the fast implementation of Eigen [40] leveraging block operations.

#### F. Mehrotra's predictor corrector algorithm

As much as we have reduced the computational complexity of the Newton's method it is still key to keep the overall number of Newton iterations at a minimum. A very effective measure is Mehrotra's predictor-corrector algorithm [43] which enables fast convergence by choosing  $\sigma_{\mathcal{A}_{l-1}^{\mathcal{A}_{l-1}}}$  and  $\sigma_{l,i}$  appropriately. The algorithm for LSP is described in [44] (Alg. 16.4) and only requires slight adaptations for HLSP which are detailed in Appendix D.

Even though the primal ( $O(n_r^2)$ ) needs to be computed twice per Newton iteration (and the dual only once ( $O(\underline{m}_{\mathcal{A}_{l-1}^{\mathcal{A}_{l-1}}})$ ) for the corrector step if required by the convergence test, see sec. III-D) this effort is negligible in comparison to the

---

**Algorithm 1** Primal-dual NIPM-HLSP

---

```
1: procedure INTPTHLSPP( $p, \underline{A}_p, \underline{b}_p$ )
2:   rank = 0
3:   for l=1:p do
4:     while  $\|K_l\|_2 > \epsilon$  & iter < maxIter do
5:       CalcDualAndPrimalStep(predictor)
6:       CalcDualAndPrimalStep(corrector)
7:       Make step with  $\_ = \_ + \alpha \Delta \_$  for new  $x, w_{l,i},$ 
          $v_{l,i}, \underline{w}_{\underline{A}_{l-1}^\xi}, \underline{\lambda}_{\underline{A}_{l-1}^\xi, l}$ 
8:       if  $l > 1$  then
9:         If required by the convergence test in
         sec. III-D, compute the dual  $\underline{\lambda}_{\underline{A}_{l-1}, l}$  with (66)
10:      end if
11:    end while
12:    project(inactive)
13:    if rank  $\geq n$  then return  $x, \underline{\lambda}_{\underline{A}_p, p}$  end if
14:    project(current)
15:    if rank  $\geq n$  then return  $x, \underline{\lambda}_{\underline{A}_p, p}$  end if
16:  end for
17:  return  $x, \underline{\lambda}_{\underline{A}_p, p}$ 
18: end procedure
```

---

---

**Algorithm 2** Primal-dual NIPM-HLSP

---

```
1: procedure CALCPRIMALANDDUALSTEP(type)
2: if type == predictor then
3:   Solve (24) or (30) (if  $\underline{m}_{\underline{A}_{l-1}^\xi} + m_{l,i} + 2m_{l,e} < n_r$ ) for the
   affine primal step  $\Delta z$  with  $\sigma_{l,i} = \sigma_{\underline{A}_{l-1}^\xi} = 0$  and (55)
4: else
5:   Solve (24) or (30) (if  $\underline{m}_{\underline{A}_{l-1}^\xi} + m_{l,i} + 2m_{l,e} < n_r$ ) for the
   centered primal step  $\Delta z$  with  $\sigma$  as in (63) and with (67).
6: end if
7:  $\Delta x = N_{l-1} \Delta z$ 
8: Calculate  $\Delta v_{l,i}, \Delta w_{l,i}, \Delta \underline{w}_{\underline{A}_{l-1}^\xi}, \Delta \underline{\lambda}_{\underline{A}_{l-1}^\xi}$  with  $\Delta x$ 
9: Line search for  $\alpha$  on  $v_{l,i} \leq 0, w_{l,i} \geq 0, \underline{w}_{\underline{A}_{l-1}^\xi} \geq 0$  and
    $\underline{\lambda}_{\underline{A}_{l-1}^\xi} \geq 0$ .
10: end procedure
```

---

cost of the QR decomposition ( $O(4/3n_r^3)$ ) which needs to be conducted fewer times due to the improved convergence of Mehrotra's algorithm.

#### IV. ALGORITHM FOR IPM-HLSP

Algorithms 1, 2 and 3 give a comprehensive overview of an efficient implementation of the IPM-HLSP. Algorithm 1 describes the overall routine while alg. 2 details the predictor and corrector step calculation and alg. 3 details the active set compositions and projections. A simplified overview is given below:

- Go through the hierarchy from level 1 to  $p$
- For each level  $l$ , conduct the hierarchical Newton's method
- Upon convergence of the Newton's method, gather all inactive inequality constraints from higher priority levels  $\underline{A}_{l-1}^\xi$  that are saturated and add them to the active set of the virtual priority level  $l^*$ .

---

**Algorithm 3** Primal-dual NIPM-HLSP

---

```
1: procedure PROJECT(type)
2: if type == inactive then
3:   Gather active set  $\mathcal{A}_{l^*}$  from constraints in  $\underline{A}_{l-1}^\xi$  if  $\underline{w}_{\underline{A}_{l-1}^\xi} \leq$ 
      $\xi$  and  $\underline{\lambda}_{\underline{A}_{l-1}^\xi} \geq \xi$ 
4:   Calculate  $Z_{l^*}$  of  $A_{\mathcal{A}_{l^*}} N_{l-1}$  and project such that  $N_{l^*} =$ 
      $N_{l-1} Z_{l^*}$ 
5:   rank = rank + rank( $A_{\mathcal{A}_{l^*}} N_{l-1}$ )
6: else
7:   Gather active set  $\mathcal{A}_l$  comprising of all equalities and all
     active inequalities that are active with  $v_{l,i} < -\xi$  and
      $w_{l,i} < \xi$ .
8:   Add the remaining inactive inequality constraints ( $v_{l,i} \geq$ 
      $-\epsilon$  and  $w_{l,i} \geq \xi$ ) to  $\underline{A}_{\mathcal{A}_l^\xi}$ .
9:   Calculate  $Z_l$  of  $A_{\mathcal{A}_l} N_{l^*}$  and project such that  $N_l = N_{l^*} Z_l$ 
10:  rank = rank + rank( $A_{\mathcal{A}_l} N_{l^*}$ )
11: end if
12: end procedure
```

---

- Compute its nullspace and project lower priority levels and the remaining inactive inequality constraints into it.
- Add all equalities and the violated inequality constraints from level  $l$  to the active set of level  $l$ .
- Compute its nullspace and project lower priority levels and the remaining inactive inequality constraints into it.

For more details please directly refer to the code at <https://www.github.com/pfeiffer-kai/NIPM-HLSP>.

#### V. COMPARISON OF THE OPERATION COUNTS BETWEEN THE DIFFERENT NEWTON'S METHODS

Figure 1 details the number of operations per Newton iteration for the classical (21) and projected normal equations (24) and the least squares form (30) for a LSP (i.e. a two-level hierarchy  $p = 2$ ).  $A_{1,e}$  consists of linearly independent constraints and  $C_2$  is a square full-rank matrix which is necessary in order for the Cholesky decomposition to be applied.

Each method thereby requires calculations at the beginning of the Newton's method.

For the **classical normal equations** (21) we need to precalculate  $A_{2,e}^T A_{2,e}$  in  $O(m_{2,e} n^2)$ .

For the **projected normal equations** (24) we need to precalculate the null-space basis  $Z_{1,e}$  in  $O(2m_{1,e}^2 n - 2/3m_{1,e}^3)$  and do the projections  $A_{2,e} Z_{1,e}$  ( $O(2m_{2,e} n n_r)$ ) and  $A_{1,i} Z_{1,e}$  ( $O(2m_{1,i} n n_r)$ ).  $(A_{2,e} Z_{1,e})^T (A_{2,e} Z_{1,e})$  is then calculated in  $O(m_{2,e} n^2)$ .

The **least squares form** (30) requires precalculation of the null-space basis  $Z_{1,e}$  in  $O(2m_{1,e}^2 n - 2/3m_{1,e}^3)$  and the projections  $A_{2,e} Z_{1,e}$  in  $O(2m_{2,e} n n_r)$  and  $A_{1,i} Z_{1,e}$  in  $O(2m_{1,i} n n_r)$ .

A direct comparison between the methods is difficult due to the dependency on the different factors at play (number of overall Newton iterations,  $n, m_{1,i}, m_{1,e}, \text{rank}(A_{1,e})$ ). The projected normal equations (3 steps) and the least squares form (2 steps) however require significantly less steps per Newton iteration than the classical normal equations (6 steps). If there is a sufficient number of Newton iterations this circumstance has the potential of setting off the cost of the null-space

**Classical normal equations (21)**

- 1) Form the matrix product  $A_{1,i}^T W_{1,i}^{-1} \Lambda_{1,i} A_{1,i}$  in  $O(m_{1,i} n^2)$  operations with  $A_{1,i} \in \mathbb{R}^{m_{1,i}, n}$ .
  - 2) Cholesky decomposition  $O(n^3/3)$  of  $C_2$ .
  - 3) Form matrix  $A_{1,e} C_2^{-1} A_{1,e}$  in  $O(m_{1,e} n^2 + m_{1,e}^2 n)$  operations as proposed in [38].
  - 4) Cholesky decomposition of  $A_{1,e} C_2^{-1} A_{1,e}$  ( $O(m_{1,e}^3/3)$ ).
  - 5) Calculate the dual  $\lambda_{1,e}$  in  $O(m_{1,e}^2)$  operations.
  - 6) Calculate the primal  $\Delta x$  in  $O(n^2)$  operations.
- $\sum : O(m_{1,i} n^2 + n^3/3 + m_{1,e} n^2 + m_{1,e}^2 n + m_{1,e}^3/3 + m_{1,e}^2 + n^2)$

**Projected normal equations (24)**

- 1) Form the matrix product  $(A_{1,i} Z_{1,e})^T W_{1,i}^{-1} \Lambda_{1,i} (A_{1,i} Z_{1,e})$  in  $O(m_{1,i} n_r^2)$  operations for  $A_{1,i} Z_{1,e} \in \mathbb{R}^{m_{1,i}, n_r}$ .
  - 2) QR decomposition of  $Z_{1,e}^T C_2 Z_{1,e}$  ( $O(4n_r^3/3)$ ).
  - 3) Solve in  $O(n_r^2)$  for  $\Delta z$  and project for  $\Delta x$  in  $O(nn_r)$  operations.
- $\sum : O(m_{1,i} n_r^2 + n_r^3/3 + n_r^2 + nn_r)$

**Least squares form (30)**

- 1) QR decomposition of cost  $O(2n_r^2(m_{1,i} + m_{2,e}) - 2n_r^3/3)$ .
  - 2) Solve in  $O(n_r^2)$  for  $\Delta z$  and project for  $\Delta x$  in  $O(nn_r)$  operations.
- $\sum : O(2n_r^2(m_{1,i} + m_{2,e}) - 2n_r^3/3 + n_r^2 + nn_r)$

Fig. 1: Number of operations per Newton iteration for the different IPM-LSP formulations.

calculation at the beginning of the Newton's method. Also note that the classical normal equations exhibit a high degree of sparsity if the constraint matrices are sparse. This is not the case for the projected normal equations due to our choice of dense null-space basis.

Deriving from the equality  $O(m_{1,i} n_r^2) + O(n_r^3/3) = O(2n_r^2 m - 2n_r^3/3)$  we can roughly state that the least squares form is more efficient than the projected normal equations if we have  $m_{1,i} + 2m_{2,e} < n_r$ .

Figure 2 shows the computation times (Intel(R) Core(TM) i7-9750H CPU @ 2.60GHz processor with 32 Gb of RAM) for the different IPM formulations when an equality only LSP is solved.  $n = 60$ ,  $A_{1,e}$  only contains linearly independent constraints and  $C_2$  is full rank. Both matrices are dense. In case of the projected normal equations (nf-IPM) and the least-squares form (ls-IPM) the dual  $\lambda_{1,e}$  is not calculated because the KKT norm does not need to be computed for a convergence test (equality only problems converge within one iteration since the KKT conditions are linear). For reference we also show the computation times of the solver presented in [18] which is an active-set method (ASM) based HLSP solver.

The LSP is solved faster in the classical normal equations form (clas. IPM) when there is a low number of equality constraints on the first level. Note that the clas. IPM is only applicable if  $C_2$  is full rank with  $m_{2,e} \geq n$  (hence no computation times are given otherwise). In the case of  $m_{1,e} = 0$  (see top graph) one Cholesky decomposition of  $C_2$  is sufficient to solve the unconstrained LSP to obtain the primal  $\Delta x$ . Both ls-IPM and the ASM solver apply one rank revealing QR decomposition on  $A_{2,e}$  which is about 0.1 ms slower for  $m_{2,e} = 240$ . ls-IPM can reuse this decomposition for the computation of the null-space basis  $Z_{2,e}$  since  $m_{1,i} = 0$ . nf-IPM however conducts two rank revealing QR decompositions, one on  $C_2$  and another on  $A_{2,e}$  in order to obtain a basis of

its null-space  $Z_{2,e}$  (which could be avoided since there are no further priority levels but we show it for demonstration purposes).

As the number of equality constraints  $m_{1,e}$  increases both nf-IPM and ls-IPM make up for the computation time of the null-space basis computation  $Z_{1,e}$  and projection  $A_{2,e} Z_{1,e}$  as increasingly smaller problems  $n_r < n$  need to be solved on the second level. This is in contrast to the clas. IPM where an increasingly more expensive second Cholesky decomposition of  $A_{1,e} C_2^{-1} A_{1,e}$  needs to be computed. Eventually,  $n_r = 0$  for  $m_{1,e} = n = 60$  which means that both nf-IPM and ls-IPM finish after solving the first level. Again, nf-IPM is slower than ls-IPM as it computes a rank revealing QR decomposition of  $A_{1,e}^T A_{1,e}$  for the primal and a rank revealing QR decomposition of  $A_{1,e}$  for the calculation of the basis of its null-space  $Z_{1,e}$ .

With the presence of inequality constraints the computational effort of calculating the null-space basis for the projected IPM at the beginning of the Newton's method is 'spread' over the increasing number of Newton iterations gaining some advantage with respect to the classical normal equations, see sec. VI-A.

Both ASM and ls-IPM are doing the same operations for equality only problems except that the primal  $x$  is explicitly calculated after every priority level. Since this is only a minor step we assume that the slight differences in computation times are due to their specific implementations.

In order to gauge the operational cost of the IPM and the ASM for problems with inequality constraints we give a rough approximation of the number of operations that need to be conducted by each solver. The IPM-HLSP needs to resolve the Newton's method for each level. Once it converges the null-space of its active-set has to be computed and the remaining levels need to be projected into it. The pseudo-cost



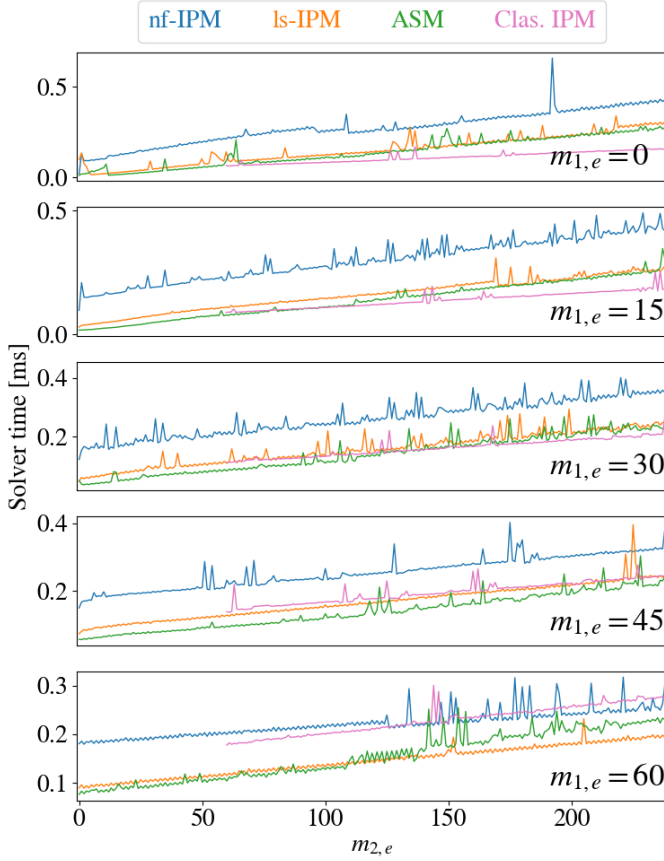


Fig. 2: Computation times of the classical and projected normal equations and the least-squares form for an equality only constrained LSP. The number of equality constraints on the first level are  $m_{1,e} = 0, 15, 30, 45, 60$  from top to bottom. The x-axis shows the number of equality constraints on the second level  $m_{2,e}$ .

then becomes

$$c_{\text{IPM-HLSP}} = \sum_{l=1}^p c_{\text{IPM}}(\text{NIter}_l, n_r, m_{\underline{A}_{l-1}^\xi} + m_{l,i}, m_{l,e}) + c_{\text{proj}}(m_{\underline{A}_l}, m_{\underline{A}_{l-1}^\xi}, m_{l+1:p}, n_r) \quad (33)$$

which is a function of  $n_r$ , the number of active constraints  $m_{\underline{A}_l}$  of each respective level, the number of inactive constraints from the previous levels  $m_{\underline{A}_{l-1}^\xi}$ , the number of equalities and inequalities of the current level  $m_{l,i}$  and  $m_{l,e}$ , the number of all equality and inequality constraints from the remaining levels  $m_{l+1:p}$  and the number of Newton iterations  $\text{NIter}_l$  of level  $l$ .

The pseudo-cost of the ASM-HLSP is composed as follows:

$$c_{\text{ASM-HLSP}} = \sum_{i=1}^{\text{ASIter}} \sum_{l=1}^p c_{\text{proj}}(m_{\underline{A}_l}, m_{l+1:p}, n_r) \quad (34)$$

ASIter are the number of active set iterations. Note that the cost of the ASM  $c_{\text{ASM}}$  is included in the projection cost (calculation of a rank revealing QR decomposition of the current level of with  $m_{\underline{A}_l}$  active constraints, projection of  $m_{l+1:p}$  constraints of the lower levels into its null-space basis). As can be seen, the null-space projection of the whole active

set needs to be repeated for each active set iteration whereas the IPM-HLSP needs to project the whole HLSP (including inactive constraints) only once per HLSP resolution. This leads to less operations for the IPM-HLSP in case of large number of active set iterations for the ASM-HLSP.

## VI. EVALUATION

In the following we evaluate our presented solver NIPM-HLSP in normal equations form (pure IPM (nf-IPM) (24) and IPM in conjunction with ASM (nf-IPM-ASM) (76)) and in least-squares form (pure IPM (ls-IPM) (30) and in conjunction with ASM (ls-IPM-ASM) (77)). We compare their performance with the IPM in classical normal equations form (21) (clas. IPM) and the ASM based HLSP solver proposed in [18] (simply referred to as ASM). The least-squares NIPM solvers are only used in the first simulation (sec. VI-A) since the number of inequality constraints usually violate the condition  $m_{\underline{A}_{l-1}^\xi} + 2m_{l,e} < n_r$  for which the least-squares form is faster. We also solve (2) with the IPM based solver GUROBI [46] and the ADMM based solver OSQP [35] over the C++ wrapper osqp-eigen. Unlike our solvers nf-IPM and nf-IPM-ASM, both these solvers are sparse solvers. We use them at standard configurations. For OSQP, warm-starting each level is disabled since the problem size can change over the course of the simulation. Since ADMM based solvers have the tendency to converge with only moderate accuracy, OSQP possesses the functionality to make an educated guess about the active set ('polishing'). We enable this functionality for the second (sec. VI-B) and third simulation (sec. VI-C).

We sample our simulations all from real-time robot control as it allows us to intentionally create numerically ill-posed problems which lead to high number of active set problems. We start with a kinematic robot control situation where the classical and projected normal equations for LSP are compared (see sec. VI-A). The evaluation is continued with a dynamic robot simulation depicting the effect of a larger number of variables and inequality constraints on the solver timings (sec. VI-B). The evaluation is concluded with a push simulation in order to observe the distinctive difference in behavior between the two solvers in case of a singular instance of a large change of the active set (sec. VI-C). For the simulations we use the HRP-2Kai humanoid robot with 38 degrees of freedom (DoF) [47].

We depict the overall solver times, the required number of iterations (for OSQP both iterations and number of factorization updates as a dashed line), the time per Newton iteration (solver time divided by number of iterations; not for ASM and OSQP) and the maximum KKT norm of all the levels. Most plots are in logarithmic scale for better readability.

The simulations are run on an Intel(R) Core(TM) i7-9750H CPU @ 2.60GHz processor with 32 Gb of RAM.

### A. Kinematic robot example - Comparing the classical and projected IPM

In the first simulation we want to demonstrate that our IPM-HLSP (24) projected into the null-space of active constraints

### Hierarchy A

- 1) • 76 inequalities as bound constraints for the lower and upper joint angle limits
  - 18 equality constraints for the geometric contact constraints of the two feet and the left hand
- 2) • 2 inequality constraints on the center of mass (CoM) in the transverse plane
  - 3 equality constraints on the position of the right hand
  - 38 regularization terms for the joint velocities

Fig. 3: Hierarchy A

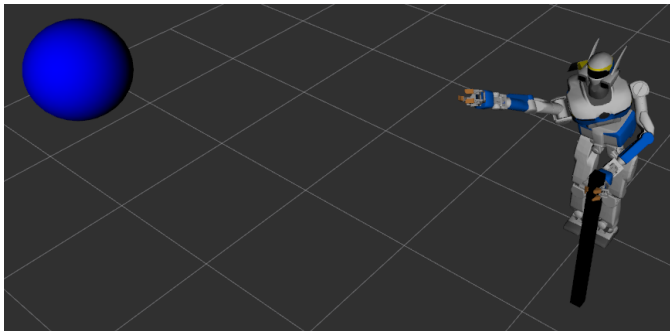


Fig. 4: HRP2 stretching into kinematic and algorithmic singularity in order to move the right hand as close as possible to the blue ball. The robot oscillates in a high frequency and low amplitude manner due to numerical instabilities.

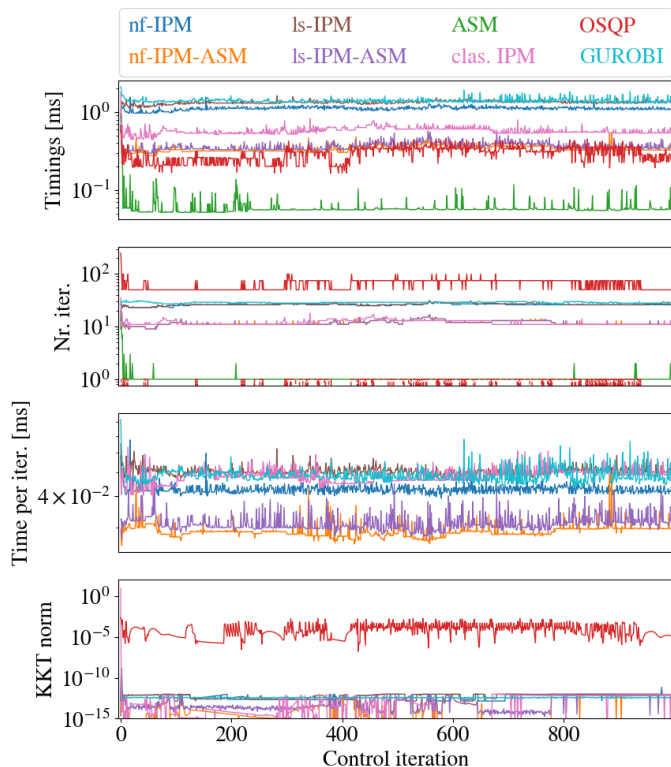


Fig. 5: Hierarchy A, fig. 3. nf-IPM-ASM and ls-IPM-ASM are about 50% faster than the clas. IPM.

can be computationally superior with respect to the clas.

IPM (21).

For this we design a stretch demonstration with the HRP-2Kai robot according to the control hierarchy A given in Fig. 3. The robot control constraints are composed of joint angle limits and geometric contact constraints for both feet to be on the ground and the left hand to be grabbing onto a pole in front of the robot. Note that the resulting  $A_{1,e}$  contains linear dependent constraints so for the clas. IPM we rely on a rank revealing QR decomposition for  $A_{1,e}C_2^{-1}A_{1,e}^T$  at cost of  $O(4/3m_{1,e}^3)$  instead of  $O(1/3m_{1,e}^3)$  for a Cholesky decomposition. The control objective is for the CoM to stay within the support polygon spanned by the feet and the right hand to reach for an out-of-reach target on the upper right of the robot. A regularization task on the joint velocities ensures the full rank property of the objective and also prevents numerically unstable robot behavior due to kinematic and algorithmic singularities. This leads to the robot taking a posture similar to the one depicted in Fig. 4 without the joint oscillations and a slightly less stretched right arm.

The results are given in Fig. 5. The top graph shows the computation times of the six different solvers while the second graph shows the ratio of their performance with respect to the one of the clas. IPM. The second graph from the bottom shows the required Newton and active set iterations to resolve the HLSP. The bottom graph shows the sum of the KKT norms of each priority level at convergence (log scale, not for ASM).

The clas. IPM is slower than the nf-IPM-ASM and ls-IPM-ASM as two decompositions per Newton iteration need to be resolved instead of one and there is a sufficiently large number of Newton iterations to make up for the cost of the null-space base computation. Consequently, and with the additional effect of variable elimination due to our choice of null-space basis, the nf-IPM-ASM is about 1.5 times as fast as the classical one. Thereby, the ls-IPM-ASM is slightly slower than the nf-IPM-ASM as  $m_{1,i} + 2m_{2,e} > n_r$ .

On the contrary, both nf-IPM and ls-IPM are clearly outperformed in terms of computation times by their ASM based siblings nf-IPM-ASM and ls-IPM-ASM due to the Newton iterations count being almost twice as high. This is reasonable as both nf-IPM and ls-IPM conduct a Newton's method to identify the initial feasible or optimal infeasible point of the first level with an unreduced number of variables. This is in contrast to nf-IPM-ASM and ls-IPM-ASM which conduct an ASM on the first level which is fast and effective due to efficient updating of the QR decomposition of  $\tilde{A}_{A_i}$  in case of possible changes of the active set. Note that in these cases null-space bases do not have to be updated as it is the case for ASM [18] or the solver presented in [17].

As fast as nf-IPM-ASM and ls-IPM-ASM are, they can not compete with the ASM which solves the problem in less than one tenth of the time of the clas. IPM due to warm starting the active set. However, identifying the initial active set in the first control iterations takes a considerable amount of active set iterations both for the ls-IPM-ASM (which implements an ASM for identifying the initial feasible or optimal infeasible point) and the ASM-HLSP. Afterwards, the LSP is mostly resolved in one active set iteration or a more or less constant number of Newton iterations in case of the IPM.

### Hierarchy B

- 1) • 152 inequality constraints for lower and upper joint angle and joint velocity limits
  - 76 lower and upper torque limits
  - 32 unilateral contact constraints for the feet
- 2) 18 equality constraints for the geometric contact constraints of the two feet and the left hand
- 3) 2 inequality constraints on the center of mass (CoM) in the transverse plane
- 4) 3 equality constraints on the position of the right hand
- 5) 38 regularization terms for the joint velocities
- 6) 36 regularization terms for the contact forces

Fig. 6: Hierarchy B

According to (2) OSQP solves two problems: firstly, finding the feasible or optimal infeasible point of the first level and secondly, resolving the second level of the hierarchy. Overall computation times are slightly faster than IPM-ASM as long as no factorization updates (dashed red line in middle graph) are required. Otherwise, both solvers require approximately the same solving time. Polishing is disabled as can be seen from the KKT norms which are constant at about  $10^{-5}$  compared to  $10^{-12}$  of the IPM based solvers.

GUROBI solves the problem in approximately the same time as ls-IPM. The time per Newton iteration ranks slightly better since GUROBI requires more iterations until convergence (due to solver settings).

The high degree of convergence of the IPM solvers shows a successful search for the feasible or optimal infeasible point on both levels by the ASM while keeping inactive constraints feasible by the IPM.

### B. Dynamic robot example - A numerically unstable robot movement

The following simulation shows the behavior of the solvers if the problem to solve is scaled up in number of variables and constraints. Also, a singular task causes highly dynamic behavior with large changes of the active unilateral contact force constraints and the joint angle, velocity and torque constraints between the control iterations. We implement the same robotic simulation setup as in sec. VI-A but this time for the dynamic control case. We include the equation of motion with 3 contact points on the two feet and the left hand. The joint torques are subsequently substituted by the equation of motion [3] such that we end up with 74 variables consisting of 38 joint velocities and 36 contact forces for the two feet and the left hand. The singular task is added to the hierarchy in form of a stretch task trying to reach for a cartesian position outside of the workspace of the robot. If such a task is not regularized [4] it leads to numerical instabilities in form of high frequency oscillations in presence of a trust region joint velocity constraint [26]. For this we integrate the joint accelerations (another possibility would be to derive the joint velocity constraint in time).

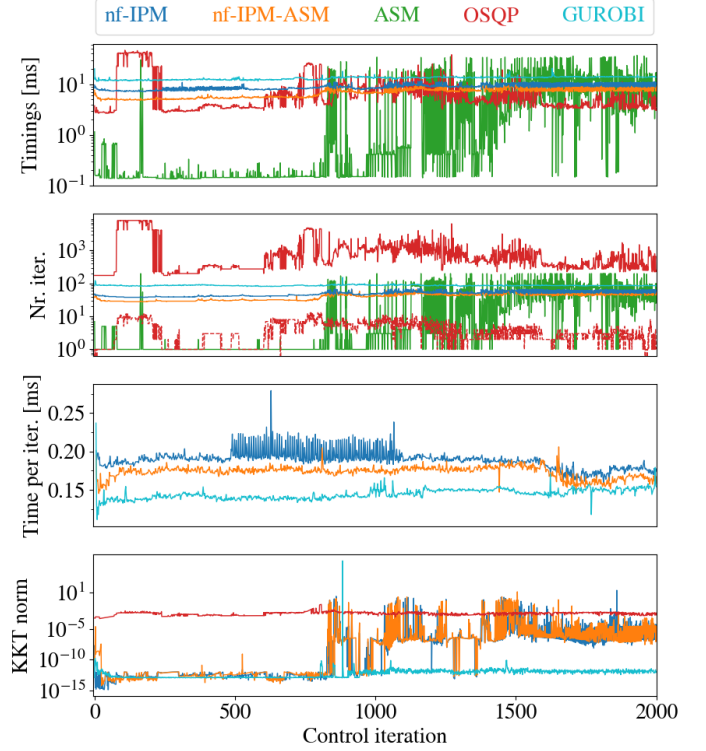


Fig. 7: Hierarchy B, fig. 6. The right arm starts stretching at control iteration 750 after which the robot behavior becomes numerically unstable.

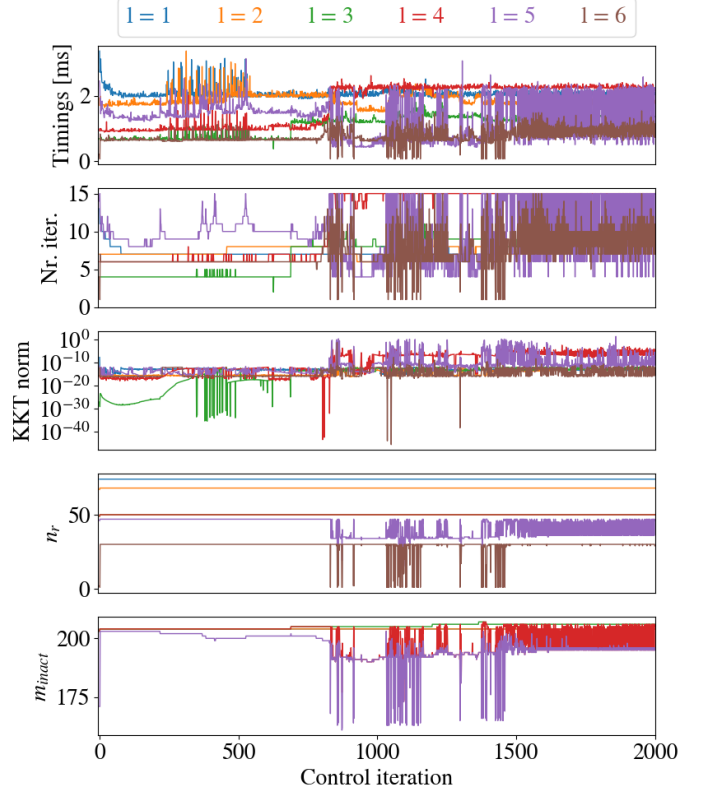


Fig. 8: Hierarchy B, fig. 6. nf-IPM's behavior for each priority level.  $n_r$  is the number of remaining variables on each respective priority level while  $m_{inact}$  corresponds to the number of inactive constraints  $m_{A_{i-1}^c}$ . Both plots are in linear scale.



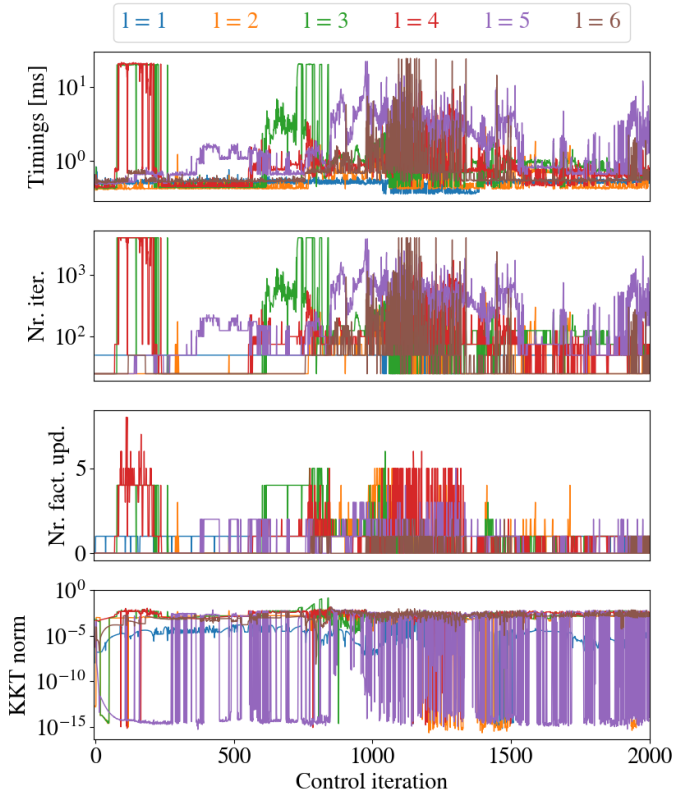


Fig. 9: Hierarchy B, fig. 6. OSQP’s behavior for each priority level. ‘Nr. fact. upd.’ (in linear scale) indicates the number of (expensive) factorization updates per priority level.

The complete control hierarchy B is given in Fig. 10.

The computation times for nf-IPM, nf-IPM-ASM, ASM, OSQP and GUROBI are given in fig. 7. nf-IPM and nf-IPM-ASM resolve the hierarchy in about 8 ms and 6 ms while the robot is numerically stable. Once the right arm starts stretching at control iteration 750 there is a slight uptick in computation times of about 2 ms due to an increased number of Newton iterations for the ill-posed arm stretch level, see fig. 8. The number of iterations per priority level is limited to 15, meaning that the fourth level converges slightly worse with a KKT norm of about  $10^{-5}$ . The fifth level suffers from similarly bad convergence with a maximum KKT norm of around 20. Nonetheless, the robot continues to behave as expected with both feet keeping contact to the ground and high frequency oscillations especially on the right arm.

GUROBI constantly shows a very high convergence rate (except for a single peak of  $1.5 \times 10^6$  due to numerical difficulties) but requires more Newton iterations to do so (around 90 compared to 40 for nf-IPM). This partly explains why the time per iteration is about 0.05ms less with respect to nf-IPM since any computational overhead gets averaged to a higher degree. On the other hand, GUROBI efficiently leverages sparsity of the constraint matrices which is not possible for nf-IPM due to dense null-space projections. Furthermore, from the second graph from the bottom of fig. 8 it can be recognized that the number of variables especially after the first level is only reduced by 8% (from 74 to 68) and may contribute to the higher computation time per iteration.

### Hierarchy C

- 1) • 152 inequality constraints for lower and upper joint angle and joint velocity limits
  - 76 lower and upper torque limits
  - 32 unilateral contact constraints for the feet
- 2) 18 equality constraints for the geometric contact constraints of the two feet and the left hand
- 3) • 3 equality constraints on the center of mass (CoM) in the transverse plane
  - 38 equality constraints in case of second order regularization
- 4) 38 regularization terms for the joint velocities
- 5) 36 regularization terms for the contact forces

Fig. 10: Hierarchy C

ASM fails to find a reasonable approximation of the true active set within the given limit of 200 iterations in many control iterations. This leads to the feet losing contact and the right arm swaying uncontrollably. Also, such a large number of active set iterations causes ASM to violate the real-time constraint with computation times of about 37 ms.

OSQP converges with a maximum KKT norm of about 0.14 on level 3. While the hierarchy is mostly resolved around 2 ms faster than by IPM-ASM there are a lot of instances where OSQP requires both a high number of iterations and factorization updates. This leads to computation times of up to 42 ms (8175 iterations, 9 factorization updates). We observed that it is quite hard to maintain feasibility of the subsequent LSP’s of (2) due to the inherent moderate convergence accuracy of the ADMM. As can be seen from the KKT norms in fig. 9 there is always a level where the polishing process would fail such that the corresponding level converges at about  $10^{-3}$ . This negatively influences the determination of the optimal infeasible points. While this may be acceptable for LSP’s it is problematic for HLSP’s since wrongly determined violations  $v_{A_{l-1}}^*$  render the subsequent priority levels infeasible and eventually lead to solver failure and numerical difficulties. We explicitly recalculate the violations  $v_{l,e} = A_{l,e}x - b_{l,e}$  and  $v_{l,i} = A_{l,i}x - b_{l,i}$  at convergence of each priority level which can slightly mitigate this circumstance. The design of a dedicated hierarchical ADMM solver may be able to better handle such situation.

### C. Dynamic robot example - Handling a push

While the previous example in sec. VI-B is interesting from a numerical point of view, there exist various regularization methods to prevent such numerically unstable behavior [4], [22], [26], [48]–[51]. This last example therefore looks at a situation which may occur in a real robot situation, namely handling a push. For this we use the control hierarchy C given in Fig. 10. In contrast to the previous examples we now only have one control task on the CoM as equality constraints in all three spatial directions.

The robot is asked to lower its CoM. During the process at control iteration 400 a push from behind of magnitude 800 N

## VII. CONCLUSION

With this work we have formulated an IPM-HLSP based on the null-space method which requires only a single decomposition of the KKT system per Newton iteration instead of two. This can prove computationally superior with respect to the classical IPM-LSP depending on the number of equality constraints and Newton iterations. We believe that this theoretical advancement is an important step in overcoming numerical difficulties seen with the ASM-HLSP. Our simulations showed that the IPM based solvers exhibit nearly constant number of Newton iterations throughout the simulations whereas the ASM-HLSP tends to require high number of active set iterations in dynamic or numerically unstable control situations due to ill-posed constraint matrices. Our IPM-HLSP formulation therefore may be preferred to the ASM-HLSP if solver predictability is regarded more important than very fast computation times but limited by instances of unsuccessful active set searches.

The IPM based solvers achieve very fast control performance for the kinematic control case but may be too slow for real world dynamic control applications. However, we see further potential for algorithmic improvements, for example by a sparse solver formulation, heuristically reducing the number of inactive constraints or restricting the number of Newton iterations as seen in [37]. The last point may require a primal feasible formulation (primal-barrier interior-point method) of our solver.

We believe that our formulation of the null-space method based IPM-HLSP is not only relevant for instantaneous robotic control but may also find application in other areas where the IPM is prevalent. Especially, we want to explore the possibility of applying the null-space method based IPM to MPC. Special attention requires its block diagonal structure which may be exploited for computational efficiency in our algorithm.

Another possible research direction poses the development of a dedicated ADMM solver for HLSP's. Despite the difficulties we observed for resolving hierarchies with the ADMM it converges very reliably to a moderately accurate solution. Additionally, in contrast to the IPM, ADMM solvers can be warm-started and oftentimes only require a single factorization per solver iteration.

## REFERENCES

- [1] B. Siciliano and J.-J. E. Slotine, "The general framework for managing multiple tasks in high redundant robotic systems," in *International Conference on Advanced Robotics*, 1991, pp. 1211 – 1216 vol.2.
- [2] A. Sherikov, D. Dimitrov, and P. Wieber, "Balancing a humanoid robot with a prioritized contact force distribution," in *2015 IEEE-RAS 15th International Conference on Humanoid Robots (Humanoids)*, 2015, pp. 223–228.
- [3] A. Herzog, N. Rotella, S. Mason, F. Grimmering, S. Schaal, and L. Righetti, "Momentum control with hierarchical inverse dynamics on a torque-controlled humanoid," *Autonomous Robots*, vol. 40, no. 3, pp. 473–491, Mar 2016. [Online]. Available: <https://doi.org/10.1007/s10514-015-9476-6>
- [4] S. Chiaverini, "Singularity-robust task-priority redundancy resolution for real-time kinematic control of robot manipulators," *IEEE Transactions on Robotics and Automation*, vol. 13, no. 3, pp. 398–410, 1997.
- [5] N. Mansard and F. Chaumette, "Task sequencing for high level sensor-based control," *IEEE Trans. on Robotics*, vol. 23, no. 1, pp. 60–72, 2007. [Online]. Available: <https://hal.inria.fr/inria-00350593>

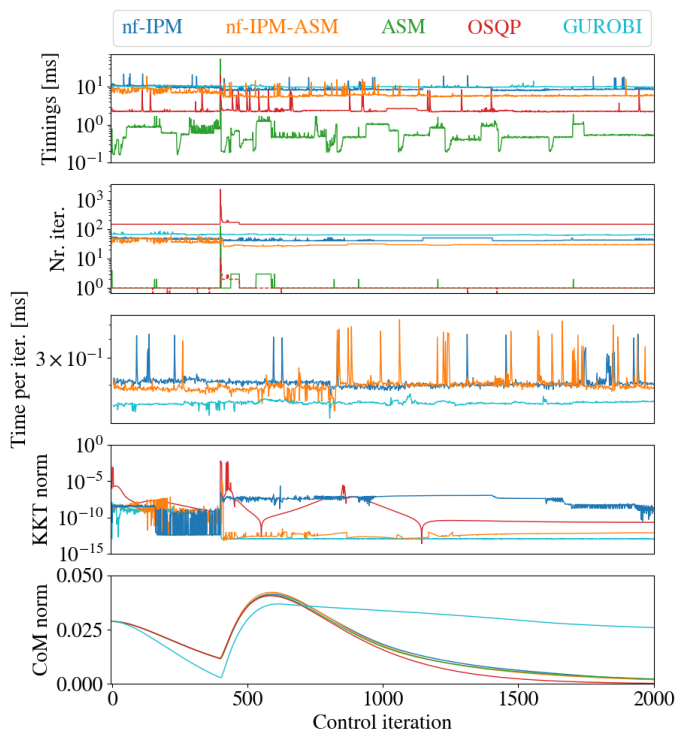


Fig. 11: Hierarchy C, fig. 10. At control iteration 400 a push from behind of magnitude 400 N is applied to the robot body.

is applied to the upper body. As can be seen from Fig. 11, this leads to a singular instance of a large number of 132 active set iterations which takes the ASM solver approximately 50 ms to resolve. We assume that this comes from an unfavorable interplay between the trust region and the joint torque limits caused by possibly ill conditioned equations of motion [52].

This also influences the convergence behavior of OSQP negatively. While OSQP manages successful polishing in most control iterations it does not do so during the push and exposes a higher KKT norm in these instances. The high number of iterations and factorization updates require around 19 ms to resolve.

In contrast, such behavior is observed only to a small degree for the IPM. As can be seen from the second and third graph from the bottom, the KKT norms and number of iterations of nf-IPM, nf-IPM-ASM and GUROBI are barely influenced. While the KKT norm of nf-IPM slightly increases in the aftermath of the push it actually decreases slightly for GUROBI. The HLSP is resolved in about 8 ms by nf-IPM-ASM with only a few peaks which can be attributed to computational artifacts of the machine running the simulation.

The push leads to the CoM of the robot being shifted to the front and increases the error norm of the CoM task as can be seen from the bottom graph. The difference in CoM behavior seen for GUROBI is due to a regularization term on the joint velocities and contact forces which amounts to the reformulated cost function  $\min_{x, v_{l,e}, v_{l,i}} \frac{1}{2} 10^{-5} \|x\|^2 + \frac{1}{2} \|v_{l,e}\|^2 + \frac{1}{2} \|v_{l,i}\|^2$ ,  $l = 1, \dots, p$  in (2). Otherwise we observed numerical difficulties.

- [6] L. Sentis and O. Khatib, "Control of free-floating humanoid robots through task prioritization," in *Proceedings of the 2005 IEEE International Conference on Robotics and Automation*, April 2005, pp. 1718–1723.
- [7] A. Liégeois, "Automatic Supervisory Control of the Configuration and Behavior of Multibody Mechanisms," *IEEE Transactions on Systems, Man, and Cybernetics*, vol. 7, no. 12, pp. 868–871, 1977.
- [8] E. Marchand and G. Hager, "Dynamic sensor planning in visual servoing," in *Proceedings. 1998 IEEE International Conference on Robotics and Automation (Cat. No.98CH36146)*, vol. 3, 1998, pp. 1988–1993 vol.3.
- [9] A. Remazeilles, N. Mansard, and F. Chaumette, "A qualitative visual servoing to ensure the visibility constraint," in *2006 IEEE/RSJ International Conference on Intelligent Robots and Systems*, 2006, pp. 4297–4303.
- [10] O. Khatib, "Real-time obstacle avoidance for manipulators and mobile robots," in *Proceedings. 1985 IEEE International Conference on Robotics and Automation*, vol. 2, 1985, pp. 500–505.
- [11] O. Kanoun, F. Lamiroux, P.-B. Wieber, F. Kanehiro, E. Yoshida, and J.-P. Laumond, "Prioritizing linear equality and inequality systems: Application to local motion planning for redundant robots," *2009 IEEE International Conference on Robotics and Automation*, no. May, pp. 2939–2944, 2009. [Online]. Available: <http://ieeexplore.ieee.org/xpls/abs/all.jsp?arnumber=5152293> <http://ieeexplore.ieee.org/lpdocs/epic03/wrapper.htm?arnumber=5152293>
- [12] Y. Abe, M. Da Silva, and J. Popović, "Multiobjective control with frictional contacts," *ACM SIGGRAPH Symposium on Computer Animation*, vol. 1, pp. 249–258, 2007.
- [13] C. Collette, A. Micaelli, C. Andriot, and P. Lemerle, "Dynamic balance control of humanoids for multiple grasps and non coplanar frictional contacts," in *IEEE/RAS International Conference on Humanoid Robots*, Pittsburgh, PA, November 29 - December 1 2007, pp. 81–88.
- [14] J. Vaillant, A. Kheddar, H. Audren, F. Keith, S. Brossette, A. Escande, K. Bouyarmane, K. Kaneko, M. Morisawa, P. Gergondet, E. Yoshida, S. Kajita, and F. Kanehiro, "Multi-contact vertical ladder climbing with an HRP-2 humanoid," *Autonomous Robots*, vol. 40, no. 3, pp. 561–580, 2016.
- [15] K. Pfeiffer, A. Escande, and A. Kheddar, "Nut fastening with a humanoid robot," in *IEEE/RSJ International Conference on Intelligent Robots and Systems (IROS)*, Sep. 2017, pp. 6142–6148.
- [16] M. De Lasa and A. Hertzmann, "Prioritized optimization for task-space control," *2009 IEEE/RSJ International Conference on Intelligent Robots and Systems, IROS 2009*, vol. 3, no. 2, pp. 5755–5762, 2009.
- [17] A. Escande, N. Mansard, and P.-B. Wieber, "Hierarchical quadratic programming: Fast online humanoid-robot motion generation," *The International Journal of Robotics Research*, vol. 33, no. 7, pp. 1006–1028, 2014.
- [18] D. Dimitrov, A. Sherikov, and P.-B. Wieber, "Efficient resolution of potentially conflicting linear constraints in robotics," Aug. 2015, submitted to IEEE TRO (05/August/2015). [Online]. Available: <https://hal.inria.fr/hal-01183003>
- [19] O. Kanoun, F. Lamiroux, and P.-B. Wieber, "Kinematic control of redundant manipulators: generalizing the task priority framework to inequality tasks," *IEEE Trans. on Robotics*, vol. 27, no. 4, pp. 785–792, 2011.
- [20] T. F. Coleman, *Large Sparse Numerical Optimization*. Berlin, Heidelberg: Springer-Verlag, 1984.
- [21] M. Benzi, G. H. Golub, and J. Liesen, "Numerical solution of saddle point problems," *Acta Numerica*, vol. 14, p. 1–137, 2005.
- [22] K. Pfeiffer, "Efficient kinematic and algorithmic singularity resolution for multi-contact and multi-level constrained dynamic robot control," Ph.D. dissertation, 12 2019.
- [23] P. Gill, S. Hammarling, W. Murray, M. Saunders, M. Wright, and S. U. C. S. O. LAB., *LSSOL (Version 1.0): a Fortran Package for Constrained Linear Least-Squares and Convex Quadratic Programming. User's Guide*. Defense Technical Information Center, 1986. [Online]. Available: <https://books.google.com/books?id=gRGotGAAAJ>
- [24] C. V. Rao, S. J. Wright, and J. B. Rawlings, "Application of interior-point methods to model predictive control," *JOURNAL OF OPTIMIZATION THEORY AND APPLICATIONS*, vol. 99, pp. 723–757, 1998.
- [25] K. Pfeiffer, A. Escande, and A. Kheddar, "Singularity resolution in equality and inequality constrained hierarchical task-space control by adaptive nonlinear least squares," *IEEE Robotics and Automation Letters*, vol. 3, no. 4, pp. 3630–3637, Oct 2018.
- [26] K. Pfeiffer, A. Escande, P. Gergondet, and A. Kheddar, "Singularity Resolution for Multi-Level Constrained Dynamically Feasible Kinematic Control," Jul. 2020, working paper or preprint. [Online]. Available: <https://hal.archives-ouvertes.fr/hal-02896719>
- [27] S. Hammarling and C. Lucas, "Updating the qr factorization and the least squares problem," 01 2008.
- [28] P. Gill, W. Murray, M. Saunders, and M. Wright, "Practical anti-cycling procedure for linearly constrained optimization," *Mathematical Programming*, vol. 45, pp. 437–474, 08 1989.
- [29] Y. Nesterov and A. Nemirovskii, *Interior-Point Polynomial Algorithms in Convex Programming*. Society for Industrial and Applied Mathematics, 1994. [Online]. Available: <https://epubs.siam.org/doi/abs/10.1137/1.9781611970791>
- [30] R. A. Bartlett, A. Wachter, and L. T. Biegler, "Active set vs. interior point strategies for model predictive control," in *Proceedings of the 2000 American Control Conference. ACC (IEEE Cat. No.00CH36334)*, vol. 6, 2000, pp. 4229–4233 vol.6.
- [31] S. Kuindersma, F. Permenter, and R. Tedrake, "An efficiently solvable quadratic program for stabilizing dynamic locomotion," in *IEEE International Conference on Robotics and Automation*, Hong Kong, China, 2014.
- [32] S. Wright, "Applying new optimization algorithms to model predictive control," in *Fifth International Conference on Chemical Process Control - CPC V*. CACHE Publications, 1997, pp. 147–155.
- [33] D. Gabay and B. Mercier, "A dual algorithm for the solution of nonlinear variational problems via finite element approximation," *Computers & Mathematics with Applications*, vol. 2, no. 1, pp. 17–40, 1976. [Online]. Available: <https://www.sciencedirect.com/science/article/pii/0898122176900031>
- [34] S. Boyd, N. Parikh, E. Chu, B. Peleato, and J. Eckstein, "Distributed optimization and statistical learning via the alternating direction method of multipliers," *Found. Trends Mach. Learn.*, vol. 3, no. 1, p. 1–122, Jan. 2011. [Online]. Available: <https://doi.org/10.1561/2200000016>
- [35] B. Stellato, G. Banjac, P. Goulart, A. Bemporad, and S. Boyd, "OSQP: an operator splitting solver for quadratic programs," *Mathematical Programming Computation*, vol. 12, no. 4, pp. 637–672, 2020. [Online]. Available: <https://doi.org/10.1007/s12532-020-00179-2>
- [36] R. J. Vanderbei, "Loqo: an interior point code for quadratic programming," *Optimization Methods and Software*, vol. 11, no. 1-4, pp. 451–484, 1999. [Online]. Available: <https://doi.org/10.1080/10556789908805759>
- [37] Y. Wang and S. Boyd, "Fast model predictive control using online optimization," *IEEE Transactions on Control Systems Technology*, vol. 18, no. 2, pp. 267–278, 2010.
- [38] A. Domahidi, A. U. Zgraggen, M. N. Zeilinger, M. Morari, and C. N. Jones, "Efficient interior point methods for multistage problems arising in receding horizon control," in *2012 IEEE 51st IEEE Conference on Decision and Control (CDC)*, 2012, pp. 668–674.
- [39] G. Frison and M. Diehl, "Hpipm: a high-performance quadratic programming framework for model predictive control\* this research was supported by the german federal ministry for economic affairs and energy (bmwi) via eco4wind (0324125b) and dyconpv (0324166b), and by dfg via research unit for 2401." *IFAC-PapersOnLine*, vol. 53, no. 2, pp. 6563–6569, 2020, 21th IFAC World Congress. [Online]. Available: <https://www.sciencedirect.com/science/article/pii/S2405896320303293>
- [40] G. Guennebaud, B. Jacob *et al.*, "Eigen v3," <http://eigen.tuxfamily.org>, 2010.
- [41] Y. Ye, M. Todd, and S. Mizuno, "An o(n)-iteration homogeneous and self-dual linear programming algorithm," *Mathematics of Operations Research - MOR*, vol. 19, 02 1994.
- [42] R. Vanderbei, *Linear Programming: Foundations and Extensions*, ser. International Series in Operations Research & Management Science. Springer US, 2013. [Online]. Available: <https://books.google.com/books?id=HjznBwAAQBAJ>
- [43] S. Mehrotra, "On the implementation of a primal-dual interior point method," *SIAM Journal on Optimization*, vol. 2, pp. 575–601, 11 1992.
- [44] J. Nocedal and S. J. Wright, *Numerical Optimization*, 2nd ed. New York, NY, USA: Springer, 2006.
- [45] A. Björck, *Numerical Methods for Least Squares Problems*. Society for Industrial and Applied Mathematics, 1996. [Online]. Available: <https://epubs.siam.org/doi/abs/10.1137/1.9781611971484>
- [46] L. Gurobi Optimization, "Gurobi optimizer reference manual," 2021. [Online]. Available: <http://www.gurobi.com>
- [47] K. Kaneko, M. Morisawa, S. Kajita, S. Nakaoka, T. Sakaguchi, R. Cisneros, and F. Kanehiro, "Humanoid robot hrp-2kai - improvement of hrp-2 towards disaster response tasks -," 11 2015.
- [48] P. Baerlocher and R. Boulic, "An inverse kinematics architecture enforcing an arbitrary number of strict priority levels," *Visual Computer*, vol. 20, no. 6, pp. 402–417, 2004.

- [49] S. R. Buss and J.-S. Kim, "Selectively damped least squares for inverse kinematics," *Journal of Graphics Tools*, vol. 10, no. 3, pp. 37–49, 2005. [Online]. Available: <https://doi.org/10.1080/2151237X.2005.10129202>
- [50] T. Sugihara, "Solvability-unconcerned inverse kinematics by the levenberg-marquardt method," *IEEE Transactions on Robotics*, vol. 27, no. 5, pp. 984–991, October 2011.
- [51] P. Harish, M. Mahmudi, B. L. Callenec, and R. Boulic, "Parallel inverse kinematics for multithreaded architectures," *ACM Trans. Graph.*, vol. 35, no. 2, pp. 19:1–19:13, Feb. 2016. [Online]. Available: <http://doi.acm.org/10.1145/2887740>
- [52] A. A. Maciejewski, "Dealing with the ill-conditioned equations of motion for articulated figures," *IEEE Computer Graphics and Applications*, vol. 10, no. 3, pp. 63–71, 1990.

## APPENDIX A

### RECURSIVE COMPUTATION OF THE LAGRANGE MULTIPLIERS ASSOCIATED WITH ACTIVE CONSTRAINTS

(25) can be rewritten to

$$\underline{A}_{\mathcal{A}_{l-1}}^T \Delta \lambda_{\mathcal{A}_{l-1}} = \begin{bmatrix} \underline{A}_{\mathcal{A}_{l-1}} \\ \underline{A}_{\mathcal{A}_{l-1}^\#} \\ A_{l,i} \\ A_{l,e} \end{bmatrix}^T \begin{bmatrix} -\lambda_{\mathcal{A}_{l-1}} \\ D \\ E \\ A_{l,e}(x + \Delta x) - b_{l,e} \end{bmatrix} \quad (35)$$

with

$$D = -\lambda_{\mathcal{A}_{l-1}^\#} - W_{\mathcal{A}_{l-1}^\#}^{-1} (\lambda_{\mathcal{A}_{l-1}^\#} \odot (b_{\mathcal{A}_{l-1}^\#} - \underline{A}_{\mathcal{A}_{l-1}^\#}(x + \Delta x)) + \sigma_{\mathcal{A}_{l-1}^\#} \mu_{\mathcal{A}_{l-1}^\#} e) \quad (36)$$

and

$$E = (I + (V_{l,i} - W_{l,i})^{-1} W_{l,i}) A_{l,i} \Delta x + A_{l,i} x - b_{l,i} - w_{l,i} + (V_{l,i} - W_{l,i})^{-1} (\sigma_{l,i} \mu_{l,i} e + w_{l,i} \odot (A_{l,i} x - b_{l,i} - w_{l,i})) \quad (37)$$

The Lagrange multipliers can be calculated recursively by

$$N_{j-1}^T A_{\mathcal{A}_j}^T \Delta \lambda_{\mathcal{A}_j} = N_{j-1}^T \left( \begin{bmatrix} \underline{A}_{\mathcal{A}_{l-1}^\#} \\ A_{l,i} \\ A_{l,e} \end{bmatrix}^T \begin{bmatrix} D \\ E \\ A_{l,e}(x + \Delta x) - b_{l,e} \end{bmatrix} - \sum_{k=j+1}^{l-1} A_{\mathcal{A}_k}^T \Delta \lambda_{\mathcal{A}_k} \right) \quad (38)$$

with  $j = l-1, \dots, 1$ . The QR decompositions of  $A_{\mathcal{A}_l} N_{l-1}$  for the calculation of the null-space basis  $Z_l$  are thereby reused.

## APPENDIX B

### DERIVING THE LEAST-SQUARES FORM OF THE IPM-HLSP

In the following we show that the projected normal equations (24) can be expressed in least squares form which avoids forming the square KKT Hessian and is solved in a more computationally efficient way in certain cases as we show in sec. V. For this we rewrite the part of the left hand side that corresponds to the inactive constraints of the previous levels  $\underline{A}_{\mathcal{A}_{l-1}^\#}$  and the equality constraints of the current level  $A_{l,e}$

$$N_{l-1}^T (A_{l,e}^T A_{l,e} + A_{\mathcal{A}_{l-1}^\#}^T W_{\mathcal{A}_{l-1}^\#}^{-1} \Lambda_{\mathcal{A}_{l-1}^\#} A_{\mathcal{A}_{l-1}^\#}) N_{l-1} \Delta z = N_{l-1}^T \begin{bmatrix} A_{\mathcal{A}_{l-1}^\#}^T \sqrt{W_{\mathcal{A}_{l-1}^\#}^{-1} \Lambda_{\mathcal{A}_{l-1}^\#}} & A_{l,e}^T \\ \sqrt{W_{\mathcal{A}_{l-1}^\#}^{-1} \Lambda_{\mathcal{A}_{l-1}^\#}} & A_{l,e}^T \end{bmatrix}^T N_{l-1} \Delta z \quad (39)$$

The right hand side is rewritten accordingly

$$\begin{aligned} & N_{l-1}^T (-A_{l,e}^T (A_{l,e} x - b_{l,e}) + \underline{A}_{\mathcal{A}_{l-1}^\#}^T \lambda_{\mathcal{A}_{l-1}^\#} + A_{\mathcal{A}_{l-1}^\#}^T F) \\ &= N_{l-1}^T (-A_{l,e}^T (A_{l,e} x - b_{l,e}) \\ &+ A_{\mathcal{A}_{l-1}^\#}^T \sqrt{W_{\mathcal{A}_{l-1}^\#}^{-1} \Lambda_{\mathcal{A}_{l-1}^\#}} \sqrt{W_{\mathcal{A}_{l-1}^\#}^{-1} \Lambda_{\mathcal{A}_{l-1}^\#}}^{-1} F) \\ &= N_{l-1}^T \begin{bmatrix} A_{\mathcal{A}_{l-1}^\#}^T \sqrt{W_{\mathcal{A}_{l-1}^\#}^{-1} \Lambda_{\mathcal{A}_{l-1}^\#}} & A_{l,e}^T \\ \sqrt{W_{\mathcal{A}_{l-1}^\#}^{-1} \Lambda_{\mathcal{A}_{l-1}^\#}}^{-1} F^T & -(A_{l,e} x - b_{l,e})^T \end{bmatrix}^T \end{aligned} \quad (40)$$

with  $N_{l-1}^T \underline{A}_{\mathcal{A}_{l-1}^\#}^T \lambda_{\mathcal{A}_{l-1}^\#} = 0$ .

The above works since  $W_{\mathcal{A}_{l-1}^\#}^{-1} \Lambda_{\mathcal{A}_{l-1}^\#} \geq 0$  per the line search and if

$$\begin{aligned} & \sqrt{W_{\mathcal{A}_{l-1}^\#}^{-1} \Lambda_{\mathcal{A}_{l-1}^\#}} \sqrt{W_{\mathcal{A}_{l-1}^\#}^{-1} \Lambda_{\mathcal{A}_{l-1}^\#}}^{-1} \\ &= \sqrt{W_{\mathcal{A}_{l-1}^\#}^{-1} \Lambda_{\mathcal{A}_{l-1}^\#}} \sqrt{W_{\mathcal{A}_{l-1}^\#} \Lambda_{\mathcal{A}_{l-1}^\#}^{-1}} = I \end{aligned} \quad (41)$$

The square root of the part of (24) corresponding to the inequality constraints of level  $l$  can be extracted as follows:

$$N_{l-1}^T A_{l,i}^T (-G + (I + (V_{l,i} - W_{l,i})^{-1} W_{l,i}) A_{l,i} N_{l-1} \Delta x) = \quad (42)$$

$$\begin{aligned} & N_{l-1}^T A_{l,i}^T \sqrt{I + (V_{l,i} - W_{l,i})^{-1} W_{l,i}} \\ & \left( \sqrt{I + (V_{l,i} - W_{l,i})^{-1} W_{l,i}}^{-1} G \right. \\ & \left. + \sqrt{I + (V_{l,i} - W_{l,i})^{-1} W_{l,i}} A_{l,i} N_{l-1} \Delta x \right) \end{aligned}$$

The expression under the square root is guaranteed to be semi-positive per the line search. We have that  $V_{1,i} - W_{1,i} \leq 0$  because of the dual feasibility conditions (10). This leads to

$$\begin{aligned} I + (V_{1,i} - W_{1,i})^{-1} W_{1,i} &\geq 0 \\ W_{1,i} &\leq -V_{1,i} + W_{1,i} \\ V_{1,i} &\leq 0 \end{aligned} \quad (43)$$

which is true and ensured by line search.

The resulting least-squares form of the IPM-HLSP is given in (30).

## APPENDIX C

### AN EFFICIENT RRQR OF THE LEAST SQUARES NEWTON'S METHOD

Here we present an efficient rank revealing QR decomposition (RRQR) of

$$\begin{bmatrix} B \\ A \end{bmatrix} := \begin{bmatrix} \sqrt{W_{\mathcal{A}_{l-1}^\#}^{-1} \Lambda_{\mathcal{A}_{l-1}^\#}} \tilde{A}_{\mathcal{A}_{l-1}^\#} \\ \sqrt{I + (V_{1,i} - W_{1,i})^{-1} W_{1,i}} \tilde{A}_{l,i} \\ \tilde{A}_{l,e} \end{bmatrix} \quad (44)$$

of (30) which leverages the triangular structure of a pre-computed QR decomposition of  $A := \tilde{A}_{l,e}$ . Thereby we used the notation  $\tilde{M} := M N_{l-1}$ .

We use the fact that  $\tilde{A}_{l,e}$  does not change over the course of the iterations of the Newton's method. We therefore can precompute a RRQR of  $\tilde{A}_{l,e}$  only once at the beginning of

the Newton's method (we refer to it as stage 1 or St1 of the overall QR decomposition):

$$A = Q_1 \begin{bmatrix} R_1 & T_1 \\ 0 & 0 \end{bmatrix} \begin{bmatrix} P_1^T \\ P_2^T \end{bmatrix} \quad (45)$$

The matrix to decompose in each Newton iteration becomes

$$\begin{bmatrix} B \\ A \end{bmatrix} = \begin{bmatrix} I & 0 \\ 0 & Q_1 \end{bmatrix} \begin{bmatrix} BP_1 & BP_2 \\ R_1 & T_1 \end{bmatrix} \begin{bmatrix} P_1^T \\ P_2^T \end{bmatrix} \quad (46)$$

Each Newton iteration then first requires stage 2 of the overall 3-step QR decomposition which consists of a non-permuted QR decomposition on the first part associated with  $R_1$ :

$$\begin{bmatrix} BP_1 \\ R_1 \end{bmatrix} = \begin{bmatrix} U_{11} & U_{12} \\ U_{21} & U_{22} \end{bmatrix} \begin{bmatrix} R_2 \\ 0 \end{bmatrix} \quad (47)$$

The computational saving is achieved by considering the upper triangular structure of  $R_1$ .

We now have

$$\begin{bmatrix} B \\ A \end{bmatrix} = \begin{bmatrix} I & 0 \\ 0 & Q_1 \end{bmatrix} \begin{bmatrix} U_{11} & U_{12} \\ U_{21} & U_{22} \end{bmatrix} \begin{bmatrix} R_2 & S_2 \\ 0 & S_3 \end{bmatrix} \begin{bmatrix} P_1^T \\ P_2^T \end{bmatrix} \quad (48)$$

with  $S_2 = U_{11}^T BP_2 + U_{21}^T T_1$  and  $S_3 = U_{12}^T BP_2 + U_{22}^T T_1$ .

Secondly, we conduct stage 3 of the process which is a permuted QR decomposition on the remaining part

$$S_3 = [V_1 \ V_2] \begin{bmatrix} R_3 & T_3 \\ 0 & 0 \end{bmatrix} \begin{bmatrix} \Pi_1^T \\ \Pi_2^T \end{bmatrix} \quad (49)$$

The overall decomposition then becomes

$$\begin{bmatrix} B \\ A \end{bmatrix} = \begin{bmatrix} I & 0 \\ 0 & Q_1 \end{bmatrix} \begin{bmatrix} U_{11} & U_{12} \\ U_{21} & U_{22} \end{bmatrix} \begin{bmatrix} I & 0 & 0 \\ 0 & V_1 & V_2 \end{bmatrix} \begin{bmatrix} R_2 & S_2 \Pi_1 & S_2 \Pi_2 \\ 0 & R_3 & T_3 \\ 0 & 0 & 0 \end{bmatrix} \begin{bmatrix} I & 0 \\ 0 & \Pi_1^T \\ 0 & \Pi_2^T \end{bmatrix} \begin{bmatrix} P_1^T \\ P_2^T \end{bmatrix} \quad (50)$$

A cheap forward substitution is now sufficient to obtain a basic solution for  $\Delta z$  of (30).

Therefore, in each Newton iteration we need to apply a QR decomposition roughly only on  $\tilde{A}_{A_{l-1}^\xi}$  since we can neglect the lower triangular zero block of  $R_1$ . Note that this RRQR does not choose the pivot elements with decreasing column norms as it is described in [45]. However, in our simulations we did not observe any adverse numerical effects by not doing so.

As a side note, we can not easily implement a separation of the form

$$\begin{bmatrix} \sqrt{W_{A_{l-1}^\xi}^{-1}} \tilde{A}_{A_{l-1}^\xi} \tilde{A}_{A_{l-1}^\xi} \\ \sqrt{I + (V_{1,i} - W_{1,i})^{-1} W_{l,i}} \tilde{A}_{l,i} \\ \tilde{A}_{l,e} \end{bmatrix} \quad (51)$$

$$= \begin{bmatrix} \sqrt{W_{A_{l-1}^\xi}^{-1}} \tilde{A}_{A_{l-1}^\xi} & 0 \\ 0 & \sqrt{I + (V_{1,i} - W_{1,i})^{-1} W_{l,i}} \\ 0 & 0 \end{bmatrix} \begin{bmatrix} \tilde{A}_{A_{l-1}^\xi} \\ \tilde{A}_{l,i} \\ \tilde{A}_{l,e} \end{bmatrix} \quad (52)$$

$$=: D \begin{bmatrix} \tilde{A}_{A_{l-1}^\xi}^T & \tilde{A}_{l,i}^T & \tilde{A}_{l,e}^T \end{bmatrix}^T \quad (53)$$

with a precomputed RRQR of  $\begin{bmatrix} \tilde{A}_{A_{l-1}^\xi}^T & \tilde{A}_{l,i}^T & \tilde{A}_{l,e}^T \end{bmatrix}^T$  since the extracted matrix  $D$  is not necessarily full rank.

## APPENDIX D

### MEHROTRA'S PREDICTOR-CORRECTOR ALGORITHM FOR IPM-HLSP

First, a decomposition of the projected normal equations (24) or the least squares form (30) is computed. Note that this only needs to be done once per Newton iteration. It is then used to first calculate the affine scaling step  $\Delta z_{\text{aff}}$ ,  $\Delta x_{\text{aff}}$ ,  $\Delta w_{l,i}^{\text{aff}}$ ,  $v_{l,i}^{\text{aff}}$ ,  $\Delta w_{A_{l-1}^\xi}^{\text{aff}}$  and  $\Delta \lambda_{A_{l-1}^\xi}^{\text{aff}}$  with

$$\sigma_{A_{l-1}^\xi} = 0 \quad (54)$$

$$F_{\text{aff}} = \lambda_{A_{l-1}^\xi} - W_{A_{l-1}^\xi}^{-1} \underline{\lambda}_{A_{l-1}^\xi} (A_{A_{l-1}^\xi} x - b_{A_{l-1}^\xi}) \quad (55)$$

$$\sigma_{l,i} = 0 \quad (56)$$

$$G_{\text{aff}} = b_{l,i} + w_{l,i} - A_{l,i} x - (V_{1,i} - W_{1,i})^{-1} W_{l,i} (A_{l,i} x - b_{l,i} - w_{l,i}) \quad (57)$$

Note that the dual  $\underline{\lambda}_{A_{l-1}^\xi}$  does not need to be computed. Line search  $\alpha_{\text{aff}}$  is conducted in order to keep the dual feasible with  $w_{l,i} + \alpha_{\text{aff}} \Delta w_{l,i}^{\text{aff}} \geq 0$ ,  $v_{l,i} + \alpha_{\text{aff}} \Delta v_{l,i}^{\text{aff}} \leq 0$ ,  $\underline{w}_{A_{l-1}^\xi} + \alpha_{\text{aff}} \Delta \underline{w}_{A_{l-1}^\xi}^{\text{aff}} \geq 0$  and  $\underline{\lambda}_{A_{l-1}^\xi} + \alpha_{\text{aff}} \Delta \underline{\lambda}_{A_{l-1}^\xi}^{\text{aff}} \geq 0$ .

With this information we calculate the corrector step  $\Delta z$ ,  $\Delta x$ ,  $\Delta v_{l,i}$ ,  $w_{l,i}$ ,  $\Delta w_{A_{l-1}^\xi}$  and  $\Delta \lambda_{A_{l-1}^\xi}$  with

$$\mu_{A_{l-1}^\xi} = \lambda_{A_{l-1}^\xi}^T w_{A_{l-1}^\xi} / m_{A_{l-1}^\xi} \quad (58)$$

$$\mu_{A_{l-1}^\xi}^{\text{aff}} = (\lambda_{A_{l-1}^\xi} + \alpha_{\text{aff}} \Delta \lambda_{A_{l-1}^\xi}^{\text{aff}})^T \quad (59)$$

$$(w_{l,A_{l-1}^\xi} + \alpha_{\text{aff}} \Delta w_{l,A_{l-1}^\xi}^{\text{aff}}) / m_{A_{l-1}^\xi}$$

$$\sigma_{A_{l-1}^\xi} = (\mu_{A_{l-1}^\xi}^{\text{aff}} / \mu_{A_{l-1}^\xi})^3 \quad (60)$$

$$\mu_{l,i} = -v_{l,i}^T w_{l,i} / m_{l,i} \quad (61)$$

$$\mu_{l,i}^{\text{aff}} = (v_{l,i} + \alpha_{\text{aff}} \Delta v_{l,i}^{\text{aff}})^T \quad (62)$$

$$(w_{l,i} + \alpha_{\text{aff}} \Delta w_{l,i}^{\text{aff}}) / m_{l,i}$$

$$\sigma_{l,i} = (\mu_{l,i}^{\text{aff}} / \mu_{l,i})^3 \quad (63)$$

For the corrector step we have

$$k_4 = v_{l,i} \odot w_{l,i} + \Delta v_{l,i}^{\text{aff}} \odot \Delta w_{l,i}^{\text{aff}} + \sigma_{l,i} \mu_{l,i} e \quad (64)$$

$$k_7 = \lambda_{A_{l-1}^\xi} \odot w_{A_{l-1}^\xi} + \Delta \lambda_{A_{l-1}^\xi}^{\text{aff}} \odot \Delta w_{A_{l-1}^\xi}^{\text{aff}} - \sigma_{A_{l-1}^\xi} \mu_{A_{l-1}^\xi} e \quad (65)$$

such that

$$D_{\text{cor}} = -\lambda_{A_{l-1}^\xi} \quad (66)$$

$$-W_{A_{l-1}^\xi}^{-1} (\lambda_{A_{l-1}^\xi} \odot (b_{A_{l-1}^\xi} - \underline{\lambda}_{A_{l-1}^\xi} (x + \Delta x)))$$

$$- \Delta \lambda_{A_{l-1}^\xi}^{\text{aff}} \odot \Delta w_{A_{l-1}^\xi}^{\text{aff}} + \sigma_{A_{l-1}^\xi} \mu_{A_{l-1}^\xi} e$$

$$F_{\text{cor}} = \lambda_{A_{l-1}^\xi} + W_{A_{l-1}^\xi}^{-1} (\lambda_{A_{l-1}^\xi} \odot (b_{A_{l-1}^\xi} - \underline{\lambda}_{A_{l-1}^\xi} x)) \quad (67)$$

$$- \Delta \lambda_{A_{l-1}^\xi}^{\text{aff}} \odot \Delta w_{A_{l-1}^\xi}^{\text{aff}} + \sigma_{A_{l-1}^\xi} \mu_{A_{l-1}^\xi} e$$

$$E_{\text{cor}} = - (I + (V_{1,i} - W_{1,i})^{-1} W_{l,i}) A_{l,i} \quad (68)$$

$$- A_{l,i} x + b_{l,i} + w_{l,i}$$

$$- (V_{1,i} - W_{1,i})^{-1} (\sigma_{l,i} \mu_{l,i} e$$

$$+ \Delta v_{l,i}^{\text{aff}} \odot \Delta w_{l,i}^{\text{aff}} + w_{l,i} \odot (A_{l,i} x - b_{l,i} - w_{l,i}))$$

$$G_{\text{cor}} = b_{l,i} + w_{l,i} - A_{l,i} x \quad (69)$$



$$-(V_{l,i} - W_{l,i})^{-1} (\sigma_{l,i} \mu_{l,i} e + \Delta w_{l,i}^{\text{aff}} \odot \Delta w_{l,i}^{\text{aff}} + w_{l,i} \odot (A_{l,i} x - b_{l,i} - w_{l,i}))$$

APPENDIX E  
THE IPM-ASM-HLSP FORMULATION

We first apply the ASM to the top three lines of (2)

$$\begin{aligned} \min_{x, v_{\mathcal{A}_l}} \quad & \frac{1}{2} \|v_{\mathcal{A}_l}\|^2 \\ \text{s.t.} \quad & A_{\mathcal{A}_l} x - b_{\mathcal{A}_l} = v_{\mathcal{A}_l} \end{aligned} \quad (70)$$

$A_{\mathcal{A}_l}$ ,  $b_{\mathcal{A}_l}$  and  $v_{\mathcal{A}_l}$  represent all equality constraints and the active inequality constraints in the active set  $\mathcal{A}_l$ .

The active set search then takes following form:

- Choose initial active set  $\mathcal{A}_l$ .
- Solve (70) for the new  $x$  and calculate  $v_{1,l} = A_{1,l} x - b_{1,l}$  (including the inactive inequality constraints)
- If there is a constraint with  $v_{1,l} < -\epsilon$  add this constraint to the active set  $\mathcal{A}_l$ . If there are several violated constraints, add the one with the largest violation  $v_{1,l}$ .
- If all constraints are saturated or satisfied, remove the constraint with the largest satisfaction  $v_{1,l} \geq \epsilon$  from  $\mathcal{A}_l$ .
- Repeat until no constraint needs to be added to or removed from the active set.

If a slightly changed problem is solved over several iterations like it is the case for instantaneous robot control we warm start the active set  $\mathcal{A}_l^{(i)}$  of the current control iteration  $i$  by adding all constraints which were active at the optimal point  $\mathcal{A}_l^{(i-1)}$  of the last control iteration  $i-1$ .

We now integrate the above development (70) into the optimization problem (2):

$$\begin{aligned} \min_{x, v_{\mathcal{A}_l}} \quad & \frac{1}{2} \|v_{\mathcal{A}_l}\|^2 \\ \text{s.t.} \quad & A_{\mathcal{A}_l} x - b_{\mathcal{A}_l} = v_{\mathcal{A}_l} \\ & \underline{A}_{\mathcal{A}_{l-1}} x - \underline{b}_{\mathcal{A}_{l-1}} = v_{\mathcal{A}_{l-1}}^* \\ & A_{\mathcal{A}_{l-1}^{\notin}} x - b_{\mathcal{A}_{l-1}^{\notin}} \geq 0 \end{aligned} \quad (71)$$

This form is very similar to (3) except that inactive inequality constraints of  $A_{l,i}$  are not considered by means of the IPM. Instead, all equality constraints  $A_{l,e}$  and the active inequality constraints are summarized in  $A_{\mathcal{A}_l}$ . Accordingly, the further developments are closely related to the one of the pure IPM-HLSP only that all entries related to  $l, i$  are removed and the index change  $l, e \rightarrow \mathcal{A}_l$  is applied.

For the augmented system we then have

$$\begin{bmatrix} C_l & -\underline{A}_{\mathcal{A}_{l-1}}^T \\ -\underline{A}_{\mathcal{A}_{l-1}} & 0 \end{bmatrix} \begin{bmatrix} \Delta x \\ \Delta \lambda_{\mathcal{A}_{l-1}} \end{bmatrix} = \begin{bmatrix} r_1 \\ r_2 \end{bmatrix} \quad (72)$$

with

$$C_l = A_{\mathcal{A}_l}^T A_{\mathcal{A}_l} + \underline{A}_{\mathcal{A}_{l-1}}^T \underline{W}_{\mathcal{A}_{l-1}}^{-1} \underline{\Lambda}_{\mathcal{A}_{l-1}} \underline{A}_{\mathcal{A}_{l-1}}$$

The right hand side is given by

$$r_1 = \underline{A}_{\mathcal{A}_{l-1}}^T \lambda_{\mathcal{A}_{l-1}} + \underline{A}_{\mathcal{A}_{l-1}}^T F + A_{\mathcal{A}_l}^T (b_{\mathcal{A}_l} - A_{\mathcal{A}_l} x) \quad (73)$$

$$r_2 = \underline{A}_{\mathcal{A}_{l-1}} x - \underline{b}_{\mathcal{A}_{l-1}} - \underline{w}_{\mathcal{A}_{l-1}}^* \quad (74)$$

with

$$F = \lambda_{\mathcal{A}_{l-1}^{\notin}} + W_{\mathcal{A}_{l-1}^{\notin}}^{-1} (\lambda_{\mathcal{A}_{l-1}^{\notin}} \odot (b_{\mathcal{A}_{l-1}^{\notin}} - \underline{A}_{\mathcal{A}_{l-1}^{\notin}} x) + \sigma_{\mathcal{A}_{l-1}^{\notin}} \mu_{\mathcal{A}_{l-1}^{\notin}} e) \quad (75)$$

The normal equations form is

$$N_{l-1}^T C_l N_{l-1} \Delta z = N_{l-1}^T r_1 \quad (76)$$

The least-squares form of the IPM-ASM-HLSP is

$$\begin{aligned} \min_{\Delta z} \quad & \left\| \begin{bmatrix} \sqrt{W_{\mathcal{A}_{l-1}^{\notin}}^{-1} \underline{\Lambda}_{\mathcal{A}_{l-1}^{\notin}} \tilde{A}_{\mathcal{A}_{l-1}^{\notin}}} \\ \tilde{A}_{\mathcal{A}_l} \end{bmatrix} \Delta z \right. \\ & \left. - \begin{bmatrix} \sqrt{W_{\mathcal{A}_{l-1}^{\notin}}^{-1} \underline{\Lambda}_{\mathcal{A}_{l-1}^{\notin}} F} \\ b_{\mathcal{A}_l} - A_{\mathcal{A}_l} x \end{bmatrix} \right\|^2 \end{aligned} \quad (77)$$

Note that the QR decomposition of  $\tilde{A}_{\mathcal{A}_l}$  can be cheaply updated in case of active set changes if the special rank revealing QR decomposition is to be used (sec. C) (no updates of null-space bases necessary).